Bull Math Biol (2012) 74:769–802
DOI 10.1007/s11538-011-9674-0

ORIGINAL ARTICLE

Synchrony and Asynchrony for Neuronal Dynamics Defined on Complex Networks

R.E. Lee DeVille · Charles S. Peskin

Received: 15 December 2009 / Accepted: 14 June 2011 / Published online: 14 July 2011

Abstract We describe and analyze a model for a stochastic pulse-coupled neuronal network with many sources of randomness: random external input, potential synaptic failure, and random connectivity topologies. We show that different classes of network topologies give rise to qualitatively different types of synchrony: uniform (Erdős–Rényi) and "small-world" networks give rise to synchronization phenomena similar to that in "all-to-all" networks (in which there is a sharp onset of synchrony as coupling is increased); in contrast, in "scale-free" networks the dependence of synchrony on coupling strength is smoother. Moreover, we show that in the uniform and small-world cases, the fine details of the network are not important in determining the synchronization properties; this depends only on the mean connectivity. In contrast, for scale-free networks, the dynamics are significantly affected by the fine details of the network; in particular, they are significantly affected by the local neighborhoods of the "hubs" in the network.

Keywords Neural network · Neuronal network · Synchrony · Mean-field analysis · Stochastic integrate-and-fire · Random graphs · Scale-free networks · Small world networks · Complex networks · Erdős–Rényi

1 Introduction

1.1 Overview

The study of synchronization of coupled nonlinear oscillators has a history that spans several centuries, starting with Huygens' observation of synchronizing pendulum

R.E.L. DeVille (✉)
University of Illinois, 1609 W. Green St., Urbana, IL 60801, USA
e-mail: rdeville@illinois.edu

C.S. Peskin
Courant Institute, 251 Mercer St., New York, NY 10012, USA

clocks (Huygens 1673). There has been a great body of work throughout this history studying such synchronization phenomena; for reviews see Strogatz (2003), Pikovsky et al. (2003), Winfree (2001). In neuroscience, it is of particular interest to investigate the dynamics of pulse-coupled nonlinear oscillators, namely, oscillators that interact only when one of them "fires." In abstract terms, this means that there is only one particular phase of an oscillator's cycle during which it has the opportunity to influence the other oscillators to which it is coupled. Typically, this influence consists of an advance or retardation in phase of the oscillator that is on the receiving end of the interaction.

There has also been much recent interest in understanding dynamical systems defined on "complex networks," sometimes defined to be random graphs whose construction depends on a complicated rule. The theory of random graphs goes back to the seminal work of Erdős and Rényi (1959, 1960) and has led to a series of deep and elegant results with connections to combinatorics, computer science, and even foundations of mathematics (Bollobás 2001; Janson et al. 2000; Alon and Spencer 2008). After it was shown that the connectivity of the Internet is well described by "scale-free" graphs (Barabási and Albert 1999; Albert and Barabási 2002), there was an explosion of interest in the applied community to understand how complex networks can model natural systems (Newman 2003), particularly in biology. The theory and simulation of dynamical systems defined on complex networks have been applied to ecology (Bascompte 2007), neuroscience (Dayan and Abbott 2001), and especially gene regulatory networks (Bower and Bolouri 2001; Wilkinson 2006; Bhan et al. 2002; Milo et al. 2002; Shmulevich et al. 2002; Zhao et al. 2005; Schlitt and Brazma 2007; Leclerc 2008).

Because of great interest in understanding the topology of networks which arise in biological applications, there have more recently been several studies of dynamical systems defined on complex networks (Barahona and Pecora 2002; Hong et al. 2002; Nishikawa et al. 2003; Lago-Fernández et al. 2000) (see in particular the excellent reviews Boccaletti et al. 2006; Arenas et al. 2008), but it is clear that there are many interesting open questions remaining. With a view toward an eventual understanding of the interactions between complex networks and complicated dynamics, we study the evolution of discrete stochastic neuronal dynamics on these networks and the propensity of these dynamics to synchronize. The authors and collaborators have studied these exact dynamics on simpler graphs in DeVille and Peskin (2008), DeVille et al. (2010), and the current work can be thought of an extension of those papers.

It is to be expected that the topology of the network determines the dynamics defined on the network, and this is what we observe below. The purpose of this paper is to understand more fully the precise dependence of the synchronization properties of neuronal dynamics on the underlying networks on which they are defined. It was shown in DeVille and Peskin (2008), DeVille et al. (2010) that random neuronal dynamics defined on "all-to-all" networks have certain interesting synchronization properties—in particular, in certain limits there exist discontinuous phase transitions between different attractors. We perform a comprehensive numerical study below, and show that, in a certain sense to be made precise below, while certain random topologies (e.g., Erdős–Rényi or "uniform" topologies; "small-world" topologies) ex-

hibit very similar behavior to the "all-to-all" networks, other topologies (e.g., "scale-free") exhibit significantly different behavior. To be more specific, we show that

- As a function of network connectivity, the transition to synchrony is quite sharp for uniform and small-world graphs (just as in the all-to-all case). For scale-free graphs, this transition is much smoother.
- For uniform and small-world graphs, the fine details of the network do not affect the overall synchronization propensities: the synchronization correlates very well with certain average properties of the network. In contrast, for scale-free graphs, the fine details of the network are important. As we see below, in many cases knowing the local neighborhood of a small number of highly connected nodes (the "hubs") of a network tells us much more than the overall average connectivity of the network.
- We observe that there is a critical parameter p_{trans} that, in most cases, is a good predictor for the synchronization of uniform and small-world graphs but does quite poorly in general for scale-free graphs. Moreover, the range of parameters for which p_{trans} fails to be a good predictor is exactly the same range of parameters where the all-to-all networks undergo a transition from synchrony to asynchrony (DeVille and Peskin 2008; DeVille et al. 2010). It was shown there that this parameter range generates to a complicated multi-phase dynamics where the network switches between synchrony and asynchrony. As long as the network is not in this "switching regime," the single parameter p_{trans} is a good predictor.
- Finally, we show that (with enough rewiring) small-world networks "look like" uniform networks in a quantifiable sense; in fact, one the rewiring parameter crosses a threshold, neuronal dynamics on small-world networks are indistinguishable from those on uniform graphs. In particular, the effect of rewiring for networks which are sparsely connected is to enhance synchronization; this is consistent with observations for other dynamical models (Barahona and Pecora 2002; Hong et al. 2002; Lago-Fernández et al. 2000). At the same time, we find that in networks which are relatively densely connected, the effect of rewiring is to reduce synchronization, which is consistent with the observations in Nishikawa et al. (2003).

1.2 Previous Work; Motivation for Current Study

Much of the work on pulse-coupled oscillators has been done in the specific context of leaky integrate-and-fire neurons; a variety of dynamics has been observed, and several authors have explained many aspects of the dynamics of these oscillators. The simplest example of an integrate-and-fire neuron is one in which the membrane potential is allowed to take values anywhere in the interval $[V_0, V_T]$; when the potential is raised to V_T, the neuron "fires" and is reset to V_0. The term "leaky" means that in the absence of external input the voltage relaxes exponentially toward V_0. It was shown by Knight (1972) that a population of uncoupled leaky integrate-and-fire neurons can be synchronized by a common periodic input. The second author of the present paper considered the case of two identical "slightly leaky" integrate-and-fire oscillators under the assumption that the firing of one oscillator gives a small upward kick to the state of the other oscillator, and showed in Peskin (1975, pp. 268–278)

that two such oscillators synchronize. The generalization to any number of oscillators, and the theorem that such a population of oscillators synchronize, was proved by Mirollo and Strogatz (1990), who, moreover, generalized the notion of "leakiness" and clarified its role in synchronization. Kuramoto (1984, 1991) introduced statistical physics approaches to understanding synchronization. Abbott and van Vreeswijk (1993), Gerstner and van Hemmen (1993), Hansel et al. (1993), Tsodyks et al. (1993), Bressloff and Coombes (1998b, 1998c, 2000), Goel and Ermentrout (2002) considered more general networks of excitable coupling on oscillatory elements and van Vreeswijk et al. (1994), Terman et al. (1998) considered the role of inhibition in synchronizing such networks. A detailed study of the time needed for synchronization was performed in Campbell et al. (1999); a general study of the effects of noise on excitable systems is in Lindner et al. (2004). Further generalization of Mirollo and Strogatz's work to a population of nonidentical pulse-coupled oscillators was considered by Senn and Urbanczik (2000/2001), who showed that deterministic networks without leakiness synchronize generically. The algebraic structure of the solutions of oscillator networks with full or partial symmetries have been studied extensively by Golubitsky, Stewart, and collaborators (Golubitsky and Stewart 1984, 1985, 1986a, 1986b, 1987, 1994, 1999a, 1999b, 2002a, 2002b, 2002c, 2005, 2006; Golubitsky et al. 1988, 1994, 1998, 2000, 2004a, 2004b, 2005, 2006; 2007; Field et al. 1991; Dellnitz et al. 1995; Dionne et al. 1995, 1996a, 1996b; Stewart et al. 2003) and by others (Bressloff et al. 1997; Bressloff and Coombes 1998a; Mirollo and Strogatz 2005, 2007; Abrams et al. 2008). Further, models (Eurich et al. 2002; Levina et al. 2007, 2009) and data (Beggs and Plenz 2003, 2004) show that neuronal networks can exhibit criticality similar to that seen in the current model.

In DeVille and Peskin (2008), the present authors introduced a model designed to explore the effect of synaptic failure on the synchronization properties of a neural network. This model (see Sect. 1.3 below for a precise definition) consists of a network of elements, each a discretized integrate-and-fire neuron that are coupled by randomly failing synapses. Whenever a neuron in this network fires, it promotes the other neurons in the network by one discrete level with some fixed probability, the synaptic probability p_{syn}. The physiological motivation for this formulation is the stochastic nature of synaptic transmission, in which the arrival of an action potential at a pre-synaptic terminal causes, with some probability, the release of a synaptic vesicle of neurotransmitter. In DeVille and Peskin (2008), the authors considered only the simplest case, without synaptic facilitation or depression, without temporal inhomogeneities, and assuming that all coupling was excitatory. It was further assumed that each neuron had to receive exactly K vesicles of neurotransmitter to bring it from reset to firing, and thus the state of each neuron is integer-valued. Immediately after firing, a neuron is reset to level 0, after which it can be promoted successively to levels $1, 2, \ldots, K$ either by the firing of other neurons or through spontaneous promotion events (caused by exogenous inputs). The network topology considered in DeVille and Peskin (2008), DeVille et al. (2010) was the simplest possible: an "all-to-all" network. Thus, whenever a neuron fired, it had an equal probability p_{syn} of raising each neuron in the network by one level. This model also incorporates refractoriness: every time a neuron fired, it could in principle start an avalanche of activity where each firing would bring other neurons up to the firing level; the refractoriness is imposed by never allowing a neuron to fire more than once in such an avalanche.

The surprising observation made in DeVille and Peskin (2008) is that such a network can support both synchronous and asynchronous dynamics *for the same parameter values*, and that the network dynamically switches between the two states. Subsequent analysis in that paper, and a much fuller analysis in DeVille et al. (2010), showed that if the networks were chosen to have many neurons, these networks can be understood as small noise perturbations of a deterministic hybrid dynamical system which possesses two attractors (by "hybrid" dynamical system we mean a dynamical system which possesses both discrete and continuous components). Dynamically, the neuronal network spends most of its time near these deterministic attractors, and switches between the two on exponentially long timescales. This hybrid system is thus a *mean-field model* for the neuronal network. Mean-field models for the dynamics of populations of neurons have been studied extensively (e.g., Knight 1972; Brunel and Hakim 1999; Sirovich 2003; Sirovich et al. 2000; Haskell et al. 2001; Cai et al. 2004, 2006; Apfaltrer et al. 2006) and typically lead to deterministic equations for an idealized "infinite number of neurons" limit. The fact that K is kept finite in the large N limit, i.e., the voltage change produced by the arrival of an action potential is not asymptotically small, is what leads to the mean-field model being a hybrid system instead of an ODE or PDE.

In summary, a network consists of N neurons, each of which requires K input events to fire, and between each pair of neurons is a faulty synapse which transmits with probability p_{syn}. In the limit $N \to \infty$, it is natural to scale the probability of synaptic success as $p_{\text{syn}} \sim N^{-1}$ so that every neuron which fires causes an $O(1)$ number of postsynaptic neurons to also fire. A rough counting argument suggests that every time a neuron fires, it will cause about $N p_{\text{syn}}/K$ other neurons to fire—if the neurons are equidistributed in their levels, we expect that about $1/K$ of them are ready to fire at any given time, and every time a neuron fires, it sends an impulse to about $N p_{\text{syn}}$ other neurons.

For a general dynamical system, we term the "reproduction rate" of an event as the number of events of similar type it gives rise to. If we have a network in which a certain class of events have an average reproduction rate more than one, then we would expect to see large cascades of activity where the number of events grows exponentially. On the other hand, if each event in a certain class has an average reproduction rate less than one, it is unlikely to see a large cascade. Let us further assume that the rules of our system are such that large cascades of activity tend to synchronize the network (e.g., consider a case where all elements caught up in such a cascade are set to the same value afterward), but that the dynamics of the network are stochastic. (The model we consider below has these properties.) Then we would expect to see the most interesting interplays between synchrony and asynchrony when the reproduction rate is near one. Moreover, if the detailed dynamics of the network allow this reproduction rate to change during the evolution of the system (for example, it could depend on the temporally-varying state of the network), then it is possible that the reproduction rate will fluctuate around one, and in fact this is the exact effect which was observed in the model of DeVille and Peskin (2008) and explained in DeVille et al. 2010—such fluctuations were responsible for the switching between synchrony and asynchrony observed there.

The arguments above suggest that in a very general context, if we choose networks and dynamics where this reproduction rate is near one but fluctuates, then we should observe interesting interplays between synchrony and asynchrony. In an "all-to-all" network of N neurons, this requires scaling the probability of synaptic success $p_{\text{syn}} \sim N^{-1}$. However, this particular limit is not entirely biologically reasonable. It is not typically true that neuronal networks are very densely connected, yet at the same time have a large probability for synaptic failure. In fact, it is more common to have networks with a somewhat sparse, *but fixed*, connectivity, and to have much more reliable (but still failure-prone) synapses. Trying to capture these aspects of network connectivity leads to the current study. In particular, it is not entirely clear a priori which parameters govern this reproduction rate, and in fact we will see that this question is complicated (we give an overview of the results in Sect. 1.5 below).

1.3 Definition of Model

In this paper, we consider neuronal dynamics on networks of neurons where the synapses have been chosen and fixed (the network is "quenched") before the dynamics are allowed to proceed. We also allow the synapses themselves to be failure-prone, meaning that whenever a neuron fires, even if a synapse is present, the postsynaptic neuron(s) receive an input with some probability less than one. We will first define the dynamics on a given network (Sect. 1.3.1), then define the families from which we will draw the networks (Sect. 1.3.2).

1.3.1 Stochastic Dynamics on the Network

Our dynamics will be determined by the quadruple $(G, K, p_{\text{syn}}, \rho)$ where

- G is a (directed) graph. Here, we use the notation that $G = (V, E)$, where $V = \{1, \ldots, N\}$ is the set of vertices in the graph, and $E \subseteq G \times G$ is the set of edges. We write $E(i, j) = 1$ or $i \to j$ iff there is an edge starting at i and ending at j. (We will typically refer to a vertex as a "neuron" and an edge as a "synapse" below, so $E(i, j) = 1$ means neuron i synapses on neuron j.) All our graphs in this paper are directed and without loops.
- $K \geq 1$ an integer, corresponding to the number of times a neuron needs to be kicked before it can fire.
- $p_{\text{syn}} \in [0, 1]$ is the *synaptic probability*, the probability of a synapse working.
- $\rho \in \mathbb{R}$ is the rate of spontaneous promotion of neurons in the network.

The state space of our network will be $S = \{0, \ldots, K-1\}^N$; choosing a point in this space specifies the voltage level of each individual neuron in the network.

The rough description of the dynamics on our network will be as follows: with rate ρ, we promote one neuron (uniformly at random) in the network. If it is raised to a level less than K, then we do nothing else and wait for the next promotion. If it hits level K, then we say it "fires", and we enter "firing mode". In firing mode, we keep track of which neurons are currently firing. Choose some neuron (say neuron i) in the firing set and promote every downstream neuron with probability p_{syn} (i.e., for every neuron j such that $E(i, j) = 1$, increment the voltage of neuron j). Stay in firing mode until the number of neurons firing is zero (note that the firing population

can both increase or decrease at any time, since neurons can be raised to firing level by kicks from other neurons). When this occurs, reset every neuron which fired to level zero. We now give a precise description:

Definition 1 (Definition of Network Dynamics) Fix the quadruple $(G, K, p_{\mathsf{syn}}, \rho)$ and choose an initial vector $X_0 \in S = (\{0, 1, \ldots, K-1\})^N$ (the initial vector X_0 can be random). Let $0 = t_0 < t_1 < \cdots$ be a sequence of times such that $t_{i+1} - t_i$ is exponentially distributed with mean $(\rho N)^{-1}$, and define X_t to be constant on $[t_i, t_{i+1})$. For each t_i, pick an index $n \in \{1, \ldots, N\}$ uniformly and compute the following:

- If $X_{t_i,n} < K-1$, then $X_{t_{i+1},n} = X_{t_i,n} + 1$, and $X_{t_{i+1},j} = X_{t_i,j}$ for all $j \neq n$, i.e., promote only neuron n by one level and leave the rest alone.
- If $X_{t_i,n} = K-1$, then define a vector $Y^{(0)}$ and two lists $F^{(0)}, G^{(0)}$, where $Y_j^{(0)} = X_{t_i,j}$ for all $j \neq n$ and $Y_n^{(0)} = K$ and $F^{(0)} = G^{(0)} = (n)$. (Think of the lists F, G as the neurons "currently firing" and "already fired," respectively.)
- Define $Y^{(k)}, F^{(k)}, G^{(k)}$ recursively: If $F^{(k)} \neq \emptyset$, we define $Z \in (\{0,1\})^N$ by

$$\begin{cases} \mathbb{P}(Z_j = 1) = p_{\mathsf{syn}},\ \mathbb{P}(Z_j = 0) = 1 - p_{\mathsf{syn}}, & \text{if } E(F_1^{(k)}, j) = 1,\ j \notin F^{(k)} \cup G^{(k)}, \\ \mathbb{P}(Z_j = 0) = 1, & \text{else.} \end{cases}$$

  Then define

$$\begin{aligned} Y^{(k+1)} &= Y^{(k)} + Z, \\ F^{(k+1)} &= \big(F^{(k)} \setminus F_1^{(k)}\big) * \big\{j \mid Y_j^{(k+1)} = K, Y_j^{(k)} < K\big\}, \\ G^{(k+1)} &= G^{(k)} * \big\{j \mid Y_j^{(k+1)} = K, Y_j^{(k)} < K\big\}, \end{aligned}$$

  where $*$ denotes the concatenation operator. In short, whenever we process the first element of the "firing list" $F^{(k)}$, we consider all other neurons in the network which are synapsed on by $F_1^{(k)}$ and which have not yet fired, and we promote them with probability p_{syn}. We then remove this neuron from $F^{(k)}$ but not $G^{(k)}$, and add those neurons which have just fired to both lists.
- Finally, define

$$k^* = \min_{k>0}\big(F^{(k)} = \emptyset\big),$$

  and

$$X_{t_{k+1},n} = \begin{cases} Y_n^{(k^*)}, & n \notin G^{(k^*)}, \\ 0, & n \in G^{(k^*)}, \end{cases}$$

  i.e., whenever the firing list is empty, we stop the cascade, set every neuron which fired back to level 0, and leave every neuron which did not fire alone. The integer k^* will be called the *size* of the cascade.

Remarks

1. The size of a cascade, k^*, must be finite, and in fact, $k^* \leq N$. At every generation of the cascade, we process one neuron, and no neuron can reenter the firing set once it has already fired. Thus, every cascade has finite size with probability 1.

2. The parameter ρ sets an overall timescale for the problem but otherwise does not affect the dynamics, and we will set $\rho = 1$ below.
3. We can think of this graph as a weighted graph where the weight on each edge is the probability p_{syn}; a more general neuronal network model could allow for a weight which was different for different edges, but we do not consider that here.

1.3.2 The Networks We Choose

The model considered in DeVille and Peskin (2008), DeVille et al. (2010) is the model described above where the graph is chosen to be the complete graph on N vertices, i.e., $E(i, j) = 1$ for all i, j. The model description is much simpler in that case, in that one need only keep track of the number of neurons at each level; in fact, this simplification was exploited in the analysis there. From above, once we specify a graph G and the other parameters, the dynamics are defined. What we want to do below is not any single graph G, but instead families of random graphs.

Definition 2 A *neuronal network model* is the quadruple $(\mathcal{G}, \mathbb{P}, K, p_{\mathsf{syn}})$, where $\mathcal{G}$ is a set of graphs, $\mathbb{P}$ a probability distribution on the set of graphs, and K, p_{syn} are as above. A graph G is chosen from $\mathcal{G}$ according to $\mathbb{P}$, and the dynamics on (G, K, p_{syn}) are then defined as above. For any observable of the dynamics on a given graph G, i.e., for any function $\phi\colon \mathcal{G} \to \mathbb{R}$, we define the *ensemble mean* (resp. *ensemble variance*) of that observable as the mean (resp. variance) of that quantity with respect to the probability distribution defined on $\mathcal{G}$, i.e.,

$$\langle \phi \rangle_{\mathbb{P}} = \sum_{G \in \mathcal{G}} \phi(G)\mathbb{P}(G), \qquad V_{\mathbb{P}}(\phi) = \left\langle \left(\phi - \langle \phi \rangle_{\mathbb{P}}\right)^2 \right\rangle_{\mathbb{P}},$$

and similarly for other moments. (It is somewhat redundant to specify $\mathcal{G}$ since it can be defined as supp $\mathbb{P}$ but we sometimes make it explicit for clarity.)

In practice, we will not explicitly give a description of $\mathcal{G}$ and $\mathbb{P}$ in closed form, but will instead describe their construction algorithmically. The choices of families we will make for $\mathcal{G}, \mathbb{P}$ in this paper will be as follows (we give a specific description of our algorithms for constructing the random graphs in Appendix below):

- $G_{\mathsf{FULL}}(N)$, the complete graph on N vertices[1] as considered in DeVille and Peskin (2008), DeVille et al. (2010). Here, $\mathbb{P}$ is a delta function on a single graph.
- $G_{\mathsf{UP}}(N, p)$, the (directed) Erdős–Rényi uniform random graph where each edge is present independently with probability p.
- $G_{\mathsf{UFE}}(N, M)$, the random graph with M edges, where the M edges are chosen without replacement uniformly from the set of $N(N-1)$ possible edges.
- $G_{\mathsf{SW}}(N, M, p_{\mathsf{rewire}})$, the Watts–Strogatz "small-world" graph (Watts and Strogatz 1998).

[1] The standard notation for the complete graph on N vertices is K_N, since we already use K for the number of levels of a neuron, we choose this nonstandard notation for the purposes of clarity.

- $G_{\mathsf{SF}}(N, M, \alpha, \beta)$, the scale-free model inspired by that of Albert and Barabási (1999) which evolves according to "preferential attachment" (although we actually use the model described in Bollobás et al. 2003).

1.3.3 Critical Parameters

The case of the complete graph on N vertices with fixed p_{syn} was considered in DeVille and Peskin (2008), DeVille et al. (2010); it was shown there that in the limit $N \to \infty$, $p_{\mathsf{syn}} N \to \beta \in (0, \infty)$, the parameter β was critical for the behavior of the limiting system, and this was intimately related to the typical reproduction rate of various events characteristic of the dynamics. As stated above, this limit is somewhat biologically unrealistic; it makes more sense to consider sparser networks with more reliable (but not perfectly reliable) synapses. The natural questions to ask are then: Are there critical parameters? What are they?

Consider a network with N neurons and M total synapses. Define

$$p_{\mathsf{edge}} = \frac{M}{N(N-1)}, \qquad p_{\mathsf{trans}} = p_{\mathsf{syn}} p_{\mathsf{edge}}.$$

We will refer to p_{edge} and p_{trans} as the "edge probability" and the "transmission probability," but strictly speaking these are only probabilities in a certain sense. Once G has been chosen, N and M are determined so that p_{edge} is a deterministic quantity and really should be thought of as the proportion of potential edges which exist. However, it is a probability in the sense that if we have a fixed graph G, and if we choose two neurons i, j uniformly at random, then there is a probability of p_{edge} that there is a synapse $i \to j$.

One might expect that the critical parameter in this model is the transmission probability p_{trans}. The argument would be as follows: pick the "average" neuron and wait until it fires. The average neuron is connected to $p_{\mathsf{edge}}(N-1)$ other neurons and will kick each of them with probability p_{syn}, so the average number of neurons kicked is $p_{\mathsf{trans}}(N-1)$. If we further assume that the population is equidistributed, then the proportion of neurons at level $K-1$ is $1/K$, so the mean number of neurons which just got kicked and which will fire is $p_{\mathsf{trans}}(N-1)/K$. Thus, we might expect the critical parameter to be p_{trans} and its critical value to be $K/(N-1) \approx K/N$. It is in these senses which we refer to as "edge probability" and "transmission probability."

The problem with the above argument is that there may be no "typical" neuron; the degree distribution of a graph will in general have a spread, so different neurons will affect the network differently. Moreover, there is nothing which guarantees equipartition, since all of the neurons in the network are correlated; in fact, in even the homogeneous case considered earlier (DeVille and Peskin 2008; DeVille et al. 2010), correlations play a role in setting up stable synchronous behavior. However, it was true in that case that $p_{\mathsf{syn}} N$ was a critical parameter in the $N \to \infty$ limit, so it is plausible that p_{trans} might play a similar role here.

1.4 Definition of Ensembles

While the parameter p_{trans} does not necessarily tell us much about a given graph, it seems the most natural first guess to characterize a given network's behavior, and

we study the efficacy of using this parameter below. What we find is that for several of the families of networks which we consider in this paper, p_{trans} is a very good quantitative predictor of a network's propensity to synchronize. To make the notion of a "good predictor" precise, we use the following framework. Assume that we have chosen a random graph model $(\mathcal{G}, \mathbb{P})$. We can consider the distribution conditioned on M or on p_{trans}, in the following way:

Definition 3 (Conditioning)

- If $\mathcal{G}$, $\mathbb{P}$, K and p_{syn} are specified, define for all $G \in \mathcal{G}$:

$$\mathbb{P}(G|M) = \begin{cases} \dfrac{\mathbb{P}(G)}{\sum_{G' \in \mathcal{G}, |E(G')|=M} \mathbb{P}(G')}, & |E(G)| = M, \\ 0, & |E(G)| \neq M. \end{cases}$$

  Note that this gives a probability distribution supported on graphs with M edges. We then choose G according to this distribution and then perform the dynamics on (G, K, p_{syn}).
- To condition on p_{trans} once $\mathcal{G}$, $\mathbb{P}$, and K are specified, we choose

$$M \in U\left(\left[p_{\text{trans}} N(N-1), N(N-1)\right] \cap \mathbb{Z}\right),$$
$$p_{\text{syn}} = p_{\text{trans}} / p_{\text{edge}} = p_{\text{trans}} N(N-1)/M.$$

  (We are using the convention that $U(S)$ for a finite set S denotes the random variable with distribution uniform on S.) Choose G according to $\mathbb{P}(\cdot|M)$ and then perform the dynamics (G, K, p_{syn}). Note that by construction we have $p_{\text{edge}}, p_{\text{syn}} \in [p_{\text{trans}}, 1]$ and $p_{\text{edge}} p_{\text{syn}} = p_{\text{trans}}$.

Definition 4 (Good Predictor) Given a triple $(\mathcal{G}, \mathbb{P}, K)$, we will say that p_{trans} is a *good predictor* for an observable ϕ if, defining $\tilde{\mathbb{P}}$ as the distribution conditioned on p_{trans}, when we compute

$$\mu_{p_{\text{trans}}} = \langle \phi \rangle_{\tilde{\mathbb{P}}}, \qquad \sigma^2_{p_{\text{trans}}} = \left\langle \left(\phi - \langle \phi \rangle_{\tilde{\mathbb{P}}}\right)^2 \right\rangle_{\tilde{\mathbb{P}}},$$

we have $\sigma_{p_{\text{trans}}}$ much smaller than $\mu_{p_{\text{trans}}}$, i.e. if it has a small coefficient of variation over the ensemble.

1.5 Summary of Results

We can now summarize the results of the paper:

- For $G_{\text{UP}}(N, p)$, $G_{\text{UFE}}(N, M)$ and for *most* parameter values, the single parameter p_{trans} is a good descriptor of the synchronization properties of the network, as defined above. The exceptions are when parameters are chosen to put the system in the region where synchrony competes with asynchrony, but this region is very small in parameter space. As shown in DeVille and Peskin (2008), DeVille et al. (2010), this is the region where $G_{\text{FULL}}(N)$ supports both synchronous and

asynchronous dynamics and switches between the two. In all cases, these random graphs also look very close to $G_{\mathsf{FULL}}(N)$ when conditioning on p_{trans}.

- For $G_{\mathsf{SW}}(N, M, p_{\mathsf{rewire}})$, we observe that if p_{rewire} is chosen above 0.5, then $G_{\mathsf{SW}}(N, M, p_{\mathsf{rewire}})$ is independent of p_{rewire} and almost indistinguishable from $G_{\mathsf{UP}}(N, p)$ or $G_{\mathsf{UFE}}(N, M)$ conditioned on the same p_{trans}. In short, with enough rewiring, small world networks look precisely like uniform networks. This is to be expected in the sense that as $p_{\mathsf{trans}} \to 1$, the model $G_{\mathsf{SW}}(N, M, p_{\mathsf{rewire}})$ becomes the model $G_{\mathsf{UFE}}(N, M)$; what is perhaps quantitatively surprising is that once about 50% of the network has been rewired, additional rewiring does not change anything. We also study small p_{rewire} below and show some interesting results specific to $G_{\mathsf{SW}}(N, M, p_{\mathsf{rewire}})$ which we describe in Sect. 4 below.
- Finally, we show that the model G_{SF} is completely unlike the other types of models. First, we will see that while the other models have a sharp transition to synchrony (i.e., as a function of p_{trans}, the networks move from asynchronous to synchronous behavior very quickly), G_{SF} has a much smoother transition. Next, we will define two candidate observables to measure synchronization, and we show that these two are well correlated on $G_{\mathsf{UP}}, G_{\mathsf{UFE}}, G_{\mathsf{SW}}$ but give quite different answers on G_{SF}. Finally, we show that even conditioning on M and p_{syn} separately (which is, of course, a stronger condition than conditioning on p_{trans} alone) does not specify the statistics of G_{SF} very well either. This means that if we choose two graphs from G_{SF} with the same number of edges, they can have significantly varying statistics. In fact, we will show that the statistics of G_{SF} are dominated by the relative strength of the "hubs" in the network, and this varies significantly over the M-edge ensemble.

In the numerics shown throughout the paper, we will always choose $N = 1000$ neurons and $K = 10$ levels from reset to firing. The effects of changing N and K were studied extensively in DeVille and Peskin (2008), DeVille et al. (2010). It was shown there that as long as K is large enough, the qualitative description of the dynamics is independent of K, so we choose $K = 10$ consistently for convenience. Also, it was shown that the typical variance of a path of these stochastic neuronal networks is N^{-1}, as would be expected, so choosing N large, but not too large, gives small-noise dynamics. This is the regime we which to study.

1.6 Organization of the Paper

In Sect. 2, we will demonstrate the similarities and differences of the different graph models, showing that the uniform and small world models are quite close, while the scale free graphs are significantly different; we will also discuss alternate metrics for measuring synchronization. In Sects. 3, 4, 5, we will discuss properties specific to the uniform, small-world, and scale-free families, respectively. Section 6 summarizes our current understanding of the model and lists some open problems and conjectures related to the model studied here. Finally, in the Appendix, we describe in detail the precise definitions of the random graphs considered in this paper.

2 Comparison of the Models

2.1 Trajectories of the Solutions

In this section, we present simulations showing the typical behavior of trajectories of all types of systems. In Fig. 1, we present some direct simulations of the neuronal network to exhibit its main two types of behavior: asynchronous and synchronous dynamics. In both cases, we have chosen a graph from $G_{\mathsf{UFE}}(N, M)$ with $N = 1000$; in frame (a) we have $M = 6000$ and in frame (b) we have $M = 10000$. Since $p_{\mathsf{syn}} = 1$ in both cases, this means $p_{\mathsf{trans}} = 6 \times 10^{-3}$ in frame (a) and $p_{\mathsf{trans}} = 1 \times 10^{-2}$ in frame (b). We will refer to these two cases as "low" and "high" coupling, giving rise to asynchronous or synchronous dynamics, respectively. What is observed for all these graphs is that they tend to synchronize more as p_{trans} increases (just as in $G_{\mathsf{FULL}}(N, M)$ as considered in DeVille and Peskin 2008; DeVille et al. 2010). Moreover, notice that the size of events is significantly different in the two cases; for low coupling the largest event is 3% of the size of the network, whereas for high coupling it is 80% over a comparable timescale. Although we only show two examples here, we find that all systems we study in this paper have similar qualitative dynamics: if p_{trans} is chosen sufficiently small, the network is asynchronous and has no large events, and if chosen sufficiently large, the network is synchronous and has large events.

What we study in the remainder of this paper is the propensity of the network to synchronize, and what we mean by this is the propensity to have events which entrain a significant fraction of the neurons in the network. One way to get a handle on this

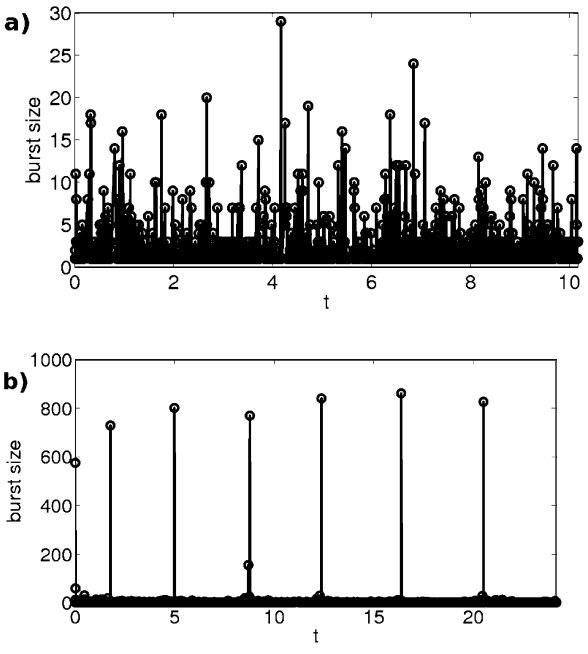

Fig. 1 Solution trajectories. Here, we show two direct simulations of neuronal network dynamics. *In both frames*, we have chosen a graph from $G_{\mathsf{UFE}}(1000, M)$, where $K = 10$ and $p_{\mathsf{syn}} = 1$. In frame (**a**), we have chosen $M = 6000$ and in frame (**b**) $M = 10000$

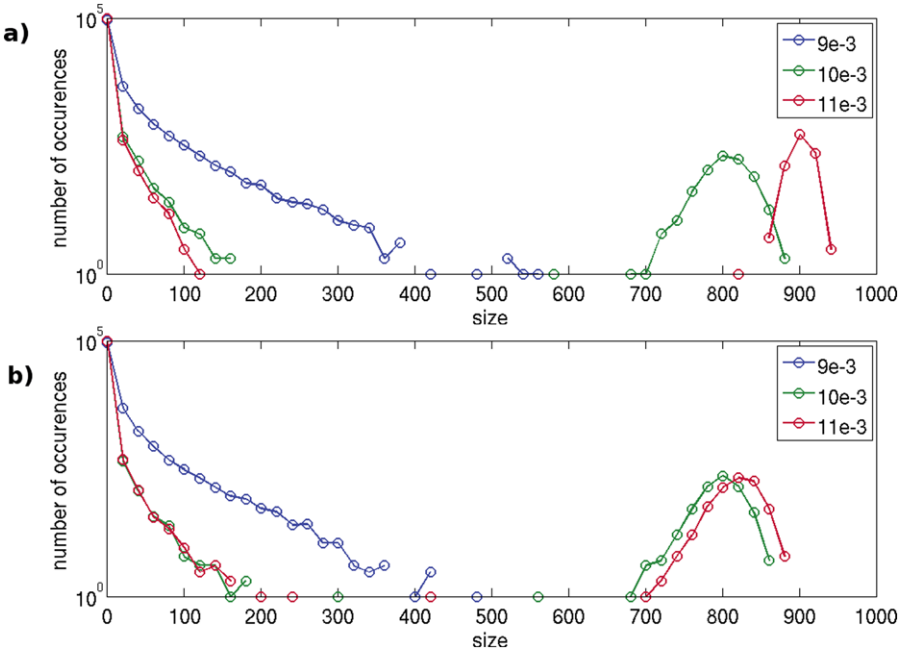

Fig. 2 (Color online) Simulations for samples of the uniform random graph $G_{\mathsf{UFE}}(N, M)$ (frame (**a**)) and $G_{\mathsf{SW}}(N, M, p_{\mathsf{rewire}})$ (frame (**b**)). *In both panels*, $N = 1000$, $K = 10$. In each case, we have chosen parameters so that $p_{\mathsf{trans}} = \{9, 10, 11\} \times 10^{-3}$. For the small world graphs in (**b**), we have chosen $p_{\mathsf{rewire}} = 0.8$

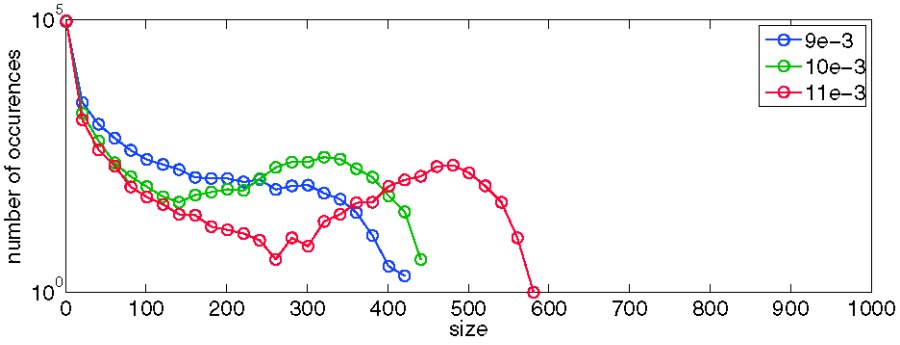

Fig. 3 (Color online) Simulations for samples of the scale-free graph $G_{\mathsf{SF}}(N, M, 1/4, 1/2)$, where $N = 1000$, $K = 10$. Again, we have chosen parameters so that $p_{\mathsf{trans}} = \{9, 10, 11\} \times 10^{-3}$

is to examine the histograms of the burst sizes when the systems are simulated over long timescales, and we present some of this data in Figs. 2 and 3.

In Fig. 2, we present histograms of burst sizes for particular graphs drawn from the $G_{\mathsf{UFE}}(N, M)$ and $G_{\mathsf{SW}}(N, M, p_{\mathsf{rewire}})$ ensembles. We have chosen three representative systems (corresponding to "low," "middle," and "high"). What happens in each case is that as we pass in parameter space from low to high is: first, there is an onset of bursts which are a significant size of the network. When $p_{\mathsf{trans}} = 9 \times 10^{-3}$,

the probability of a burst larger than half of the network is extremely low, but by $p_{\text{trans}} = 1 \times 10^{-2}$ there are many of them. As p_{trans} is increased further, the relative probabilities of the small bursts changes little, but the population of large bursts have a larger mean. We see that these are qualitatively the same for both random graph models.

In contrast, notice that Fig. 3 shows a completely different type of histogram for the scale-free networks. While the shapes undergo a transformation which is qualitatively similar (they go from monotone decreasing to developing a "hump"), that hump is centered at smaller location. Moreover, there is not a very good scale separation between the small and large events like there is in Fig. 2, and thus the histogram is smoother.

We will observe these differences throughout the remainder of the paper: the uniform and small-world models tend to act similarly and to show this sharp dichotomy between large and small events, whereas the scale-free networks have a much smoother type of dynamics, both in the scale separation between large and small for a given p_{trans} and as a function of p_{trans}.

2.2 Which Quantities to Measure?

We are interested in determining the dynamical properties of these networks and seeing how they depend on the underlying graphs. We need to collate a large amount of data and thus it makes sense to define some observables on these networks, but it is not a priori clear what the right observable is. In this section, we compare a few potential observables and justify the choices made later in the paper.

We propose three potential observables to describe the dynamics of a neuronal network: we could use the aggregate firing rate of the network, we could count the proportion of events which entrain more than a fixed proportion of the network, or we could consider the average size of the largest events.

We compare the firing rate to the other two observables in Sect. 2.3. In Fig. 4, we compare the last two potential observables: on one hand, we count the fraction of bursts which take over more than half of the network (i.e. in which more than $500 = N/2$ neurons fire), and on the other, we collect the largest 1% of all of the bursts in the network and take the mean size of these. (Stated simply, we are contrasting counting large events versus averaging the sizes of large events.) We see that for the uniform or small-world networks, it does not much matter which of these observables we choose and they correlate well. In contrast, these two observables do not correlate well at all for scale-free networks (for purposes of comparison, the same data for the uniform and small-world networks is plotted in both frames, the scale-free data has a much larger "spread"). Because we tend to see a much larger spread in the horizontal direction, we will use the counting observable: we will choose some proportion of the network size and count the proportion of bursts large than that fixed proportion.

It then remains to decide which proportion to take. For example, should we count events larger than $N/2$, or $N/5$? We make this comparison in Fig. 5, where in these graphs we always choose $p_{\text{syn}} = 1$, so $p_{\text{trans}} = p_{\text{edge}} = M/(N(N-1))$. We see that while it matters in all cases which threshold is chosen, this data underlies the difference of the scale-free networks from the other models. For the uniform and small-world networks, the distinction matters only in the regime where the network passes

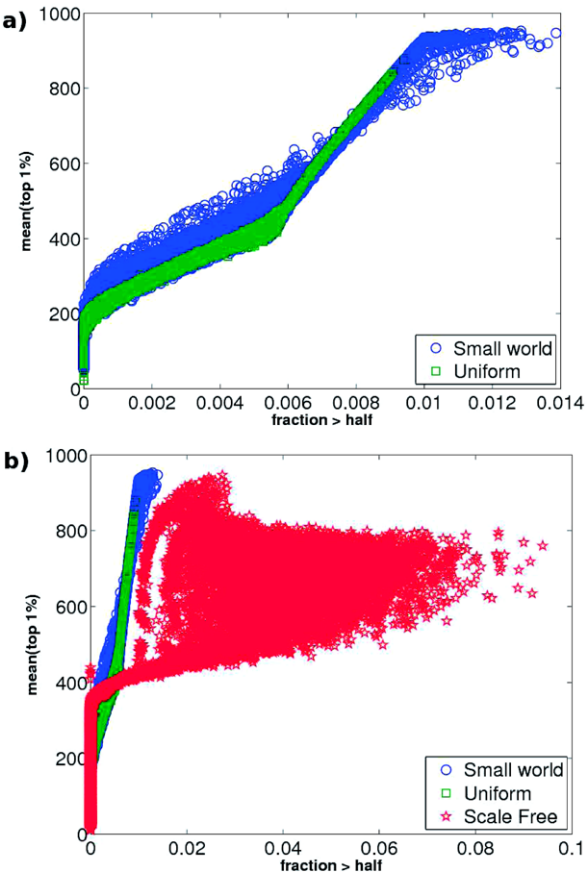

Fig. 4 (Color online) Mean size of top 1% or number above a certain threshold? Each of the data points corresponds to a realization of a random graph and the symbol specifies the distribution from which it was drawn. In all of these cases, we plot only data with $p_{\mathrm{syn}} = 1$

from zero synchronization to significant synchronization; below a certain coupling strength, there are no large events at all and both measures are zero, and above a certain coupling strength, the measures coincide, which implies that all events larger than 20% of the network are also larger than 50% of the network, consistent with the dichotomy seen in Figs. 2, 3. In contrast, the range where the two measures disagree for the scale-free networks is much larger (notice the scales on the horizontal axis; for the first three networks, the curves converge at about 10% higher value from the location where they diverge, whereas for the scale-free networks, they converge at a value about twice as high).

We also point out yet another contrast between the first three and the scale-free networks: the ensemble standard deviation. The error bars in each picture represent the ensemble standard deviation as defined in Definition 2. We see that conditioning on $p_{\mathrm{syn}}M$ (for $G_{\mathrm{FULL}}(N)$, M is fixed) gives a small ensemble standard deviation in Figs. 5(a–c), but a large one in Fig. 5(d). In fact, for the scale free networks we can see by eye that $\sigma_{p_{\mathrm{trans}}}$ is roughly half of $\mu_{p_{\mathrm{trans}}}$. We point out that this is even in light of the fact that the small-world figure contains networks with various values of p_{rewire} (although all over 0.5).

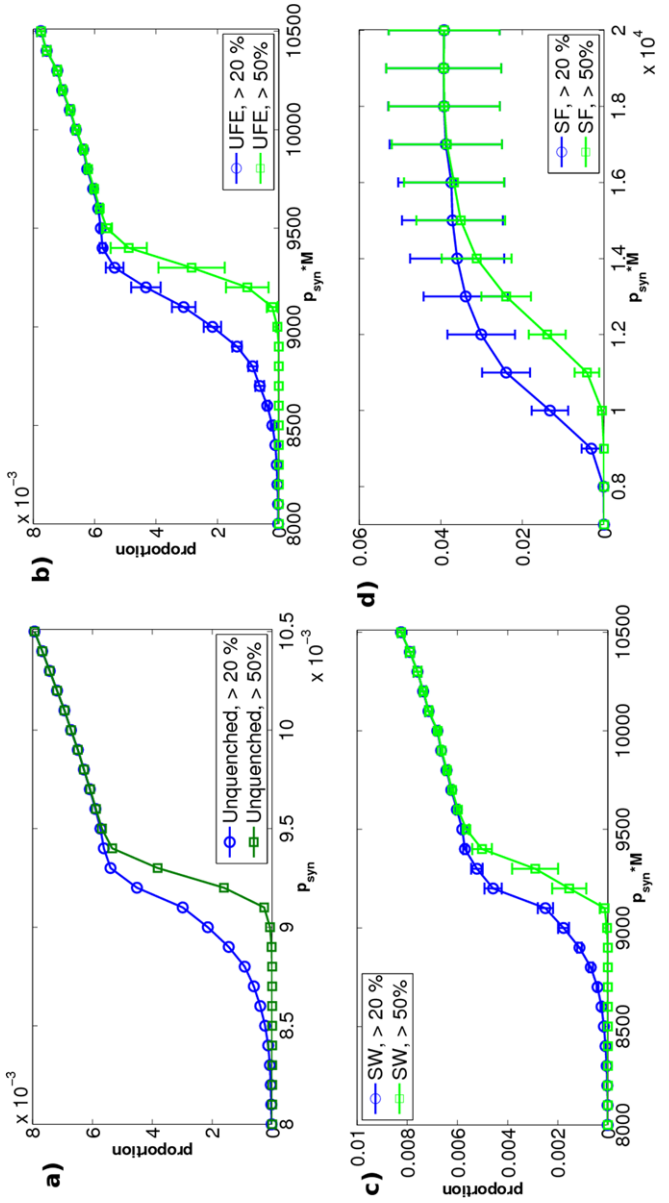

Fig. 5 (Color online) Comparing the 50% threshold with the 20% threshold. *In each plot*, we are considering a specific random graph ensemble and plotting the proportion of bursts which entrain 20% of the network and the proportion which entrain 50% of the network. The four ensembles are, in order, $G_{\mathsf{FULL}}(N)$, $G_{\mathsf{UFE}}(N, M)$, $G_{\mathsf{SW}}(N, M, p_{\mathsf{rewire}})$, $G_{\mathsf{SF}}(N, M, 1/4, 1/2)$. (Note that for G_{SW} we are choosing various values of $p_{\mathsf{rewire}} \geq 0.5$)

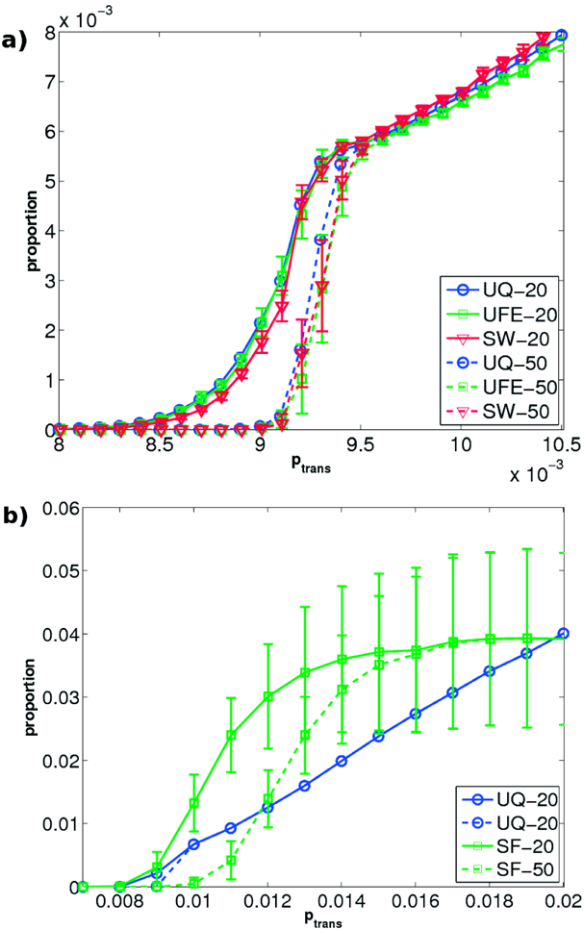

Fig. 6 (Color online) Comparing the 50% threshold with the 20% threshold across various networks. In frame (**a**), we plot all of $G_{\mathsf{FULL}}(N)$, $G_{\mathsf{UFE}}(N, M)$, $G_{\mathsf{SW}}(N, M, p_{\mathsf{rewire}})$ and see they match up nicely; in frame (**b**), we plot $G_{\mathsf{FULL}}(N)$ and $G_{\mathsf{SF}}(N, M, 1/4, 1/2)$ and see that they do not

2.3 Compare/Contrast Different Models

In Fig. 6 we aggregate information in Fig. 5 is different ways. In the left frame, we compare the 20% and 50% curves for the uniform, small-world, and complete networks. We see that if we plot all of these versus p_{trans}, then the networks match up quite well—in fact, the ensemble means are almost indistinguishable to the eye. In contrast, the scale-free networks are significantly different, and we plot this versus the complete graph. Most striking is the comparison of the range of p_{trans} where the 20% and 50% curves differ; it is an order of magnitude larger for the scale-free networks compared to the others.

In Fig. 7, we compare the aggregate firing rates of different networks; as always, the first three networks all act similarly when conditioned on p_{trans}, and the scale-free networks act quite differently. Moreover, we also see that there is a connection between firing rates and synchronization: for all cases, the aggregate firing rate rises in the region when the networks first start being synchronized, and in the uniform and small-world networks, this drops once a significant degree of synchronization

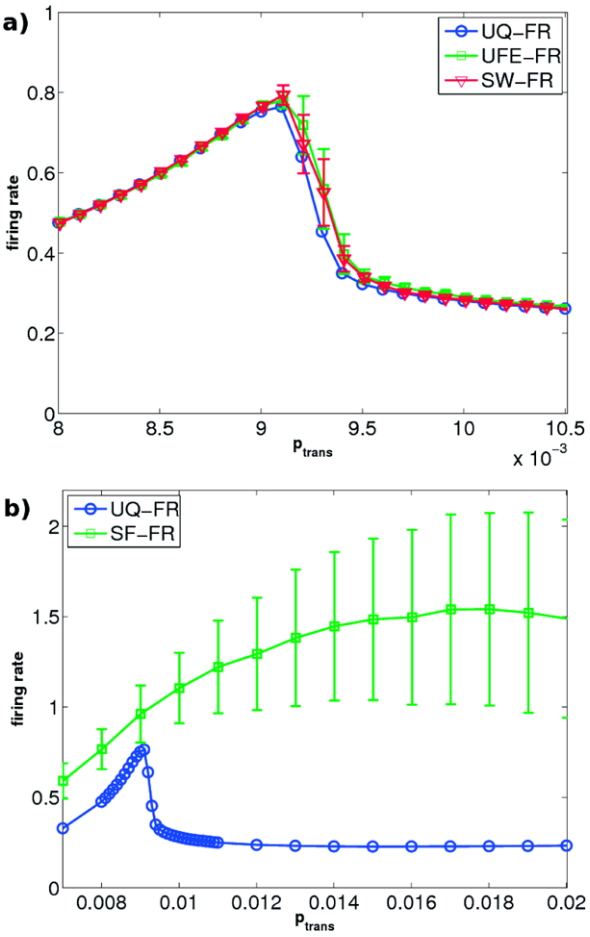

Fig. 7 (Color online) Comparing the firing rates across various networks. In frame (**a**) we plot all of $G_{\mathsf{FULL}}(N)$, $G_{\mathsf{UFE}}(N, M)$, $G_{\mathsf{SW}}(N, M, p_{\mathsf{rewire}})$ and see they match up nicely; in frame (**b**) we plot $G_{\mathsf{FULL}}(N)$ and $G_{\mathsf{SF}}(N, M, 1/4, 1/2)$ and see that they do not

takes over; however, notice that this does not happen for the scale-free case. This can be explained as follows: as was analyzed in DeVille and Peskin (2008), DeVille et al. (2010), when the $G_{\mathsf{FULL}}(N)$ system starts synchronizing to a sufficient degree, one ends up with many "wasted" firings because many of the events are $O(N)$, and during a cascade there are many cases where the same neuron is kicked several times. In this model, such neurons do not fire multiple times and end up being set to zero at the end of a cascade, so these kicks are wasted. Since the uniform and small-world networks also have these cascades which involve close to N neurons, this effect happens as well. In contrast, the scale-free networks do not exhibit such large events (see, e.g., Fig. 3), and thus there are many fewer wasted kicks. Also, we see that using aggregate firing rate as an observable for the network is not a good proxy, since it is two-to-one on almost all parameter intervals of interest. In contrast, the synchronization measures we will use are monotone over these intervals (or, more strictly speaking, their ensemble means are monotone), as can be seen in Fig. 5.

3 Detailed Study of Uniform Models

3.1 $G_{\mathsf{UP}}(N, p)$ Versus $G_{\mathsf{UFE}}(N, M)$

The first question we address here is a comparison of the $G_{\mathsf{UP}}(N, p)$ and $G_{\mathsf{UFE}}(N, M)$ models. We claim that there is not a significant difference between these two models, but $G_{\mathsf{UFE}}(N, M)$ has a slight advantage over $G_{\mathsf{UP}}(N, p)$ which we now discuss.

We present data in Fig. 8 which makes this argument; in particular, the same data is plotted in both panels of Fig. 8, but simply represented in a different way. This data was obtained in the following manner. We always choose $p_{\mathsf{syn}} = 1$ for this data. We then generated many graphs from the $G_{\mathsf{UP}}(N, p)$ distribution for various values of p; once the graph was chosen we measured the fraction of cascades larger than $N/2$, and each (background) data point is one realization of a graph. We then binned this data in p and plotted the bin mean and standard deviation; this is plotted in the solid

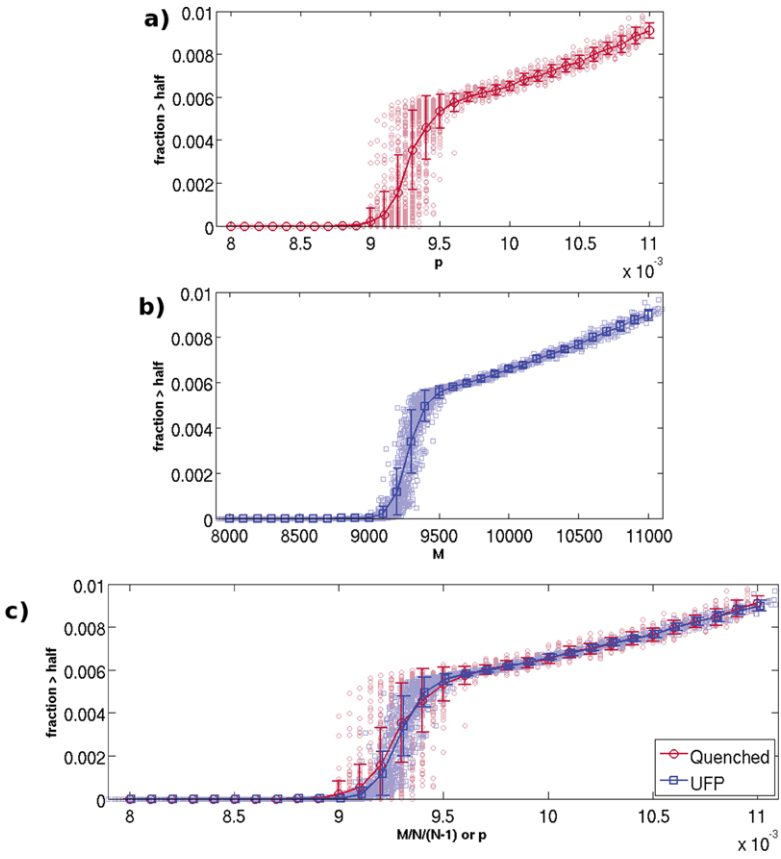

Fig. 8 (Color online) Comparison of $G_{\mathsf{UP}}(N, p)$ and $G_{\mathsf{UFE}}(N, M)$. All frames in this figure are plotting the same data, but in different ways. In frame (**a**), we plot synchronization versus p, the probability of an edge existing in a network. However, one each network has been chosen, it has a fixed number of edges M, and we can plot versus this as well. Finally, we plot all of the data in frame (**c**) against each other to show that the ensemble means are close

curve. In Fig. 8(a), everything is plotted against p, the probability of an edge existing in the random graph.

In Fig. 8(b), we plot precisely the same data, except this time plot against M, the number of edges which were actually chosen in the random graph. Again, each background data point is a single realization of the network and the solid curve is the mean and standard deviation in bins, but this time binned in M. It is clear to the eye that representing this data versus M gives a significantly lower standard deviation than representing it versus the edge probability, which indicates that, not only is knowing the number of edges useful in describing the dynamics, but in fact it is more useful than knowing the original probability p which we used to generate the random graphs.

In Fig. 8(c), we plot all of the data from Fig. 8(a, b) on top of each other to show that while the ensemble variance is different for $G_{\mathsf{UP}}(N, p)$ conditioned on p versus $G_{\mathsf{UFE}}(N, M)$ conditioned on M, the ensemble means are quite close. For any graph chosen from $G_{\mathsf{UP}}(N, p)$, the number of edges has the Bernoulli distribution with $N(N-1)$ trials and probability p of success. Since the mean of M is a function of p, and we have rescaled axes so that they match, it is not surprising that the ensemble means conditioned on p or on M give the same value. However, given p, the number of edges M has mean $N(N-1)p$ and variance $N(N-1)p(1-p)$; speaking roughly, M has mean $O(N^2)$ and standard deviation $O(N)$, which is a significant spread in absolute terms. We see that conditioning on the number M gives useful information, and in fact Fig. 8(b) suggests that this conditioning is even more useful than knowing the original p in the first place. Because of this, it seems preferable to study $G_{\mathsf{UFE}}(N, M)$ instead of $G_{\mathsf{UP}}(N, p)$, and this is what we will do below.

3.2 Comparing $G_{\mathsf{UFE}}(N, M)$ and $G_{\mathsf{FULL}}(N)$

We now compare $G_{\mathsf{UFE}}(N, M)$ and $G_{\mathsf{FULL}}(N)$ and present the data in Fig. 9. In Fig. 9(a), we compare the synchronization of $G_{\mathsf{UFE}}(N, M)$ to that of $G_{\mathsf{FULL}}(N)$ plotted versus p_{trans}. As in Fig. 8, we consider a wide variety of values for p_{syn} and M and compute the proportion of cascades larger than 50% of the network. Also as in Fig. 8, the background data points each correspond to one realization of a random graph, and we further bin in p_{trans} and plot bin mean and standard deviation. We also plot statistic for $G_{\mathsf{FULL}}(N)$ versus p_{syn} (recall that since $p_{\mathsf{edge}} = 1$ for $G_{\mathsf{FULL}}(N)$, $p_{\mathsf{syn}} = p_{\mathsf{trans}}$). The two models match well, in the sense that the ensemble mean of $G_{\mathsf{UFE}}(N, M)$ conditioned on p_{trans} is close to the actual value for $G_{\mathsf{FULL}}(N)$ for the same p_{trans}. In the $G_{\mathsf{FULL}}(N)$ model, all edges are present, but only work with probability $p_{\mathsf{syn}} = p_{\mathsf{trans}}$. One way to think of $G_{\mathsf{FULL}}(N)$ is that every time a neuron fires, one chooses a realization of $G_{\mathsf{UP}}(N, p_{\mathsf{syn}})$ and then makes the synapses downstream from the firing neuron work with probability one. In short, $G_{\mathsf{FULL}}(N)$ is dynamically averaging over realizations of graphs, whereas in the $G_{\mathsf{UP}}(N, p)$ or $G_{\mathsf{UFE}}(N, M)$ models, the graph is chosen and fixed for all time. Thus, it is to be expected that the means are close; however, it is remarkable that the ensemble variance is so small (in fact, it is almost invisible to the eye away from the onset region); in short, the effect of quenching the network before the onset of the simulation is minimal, at least outside of the switching regime.

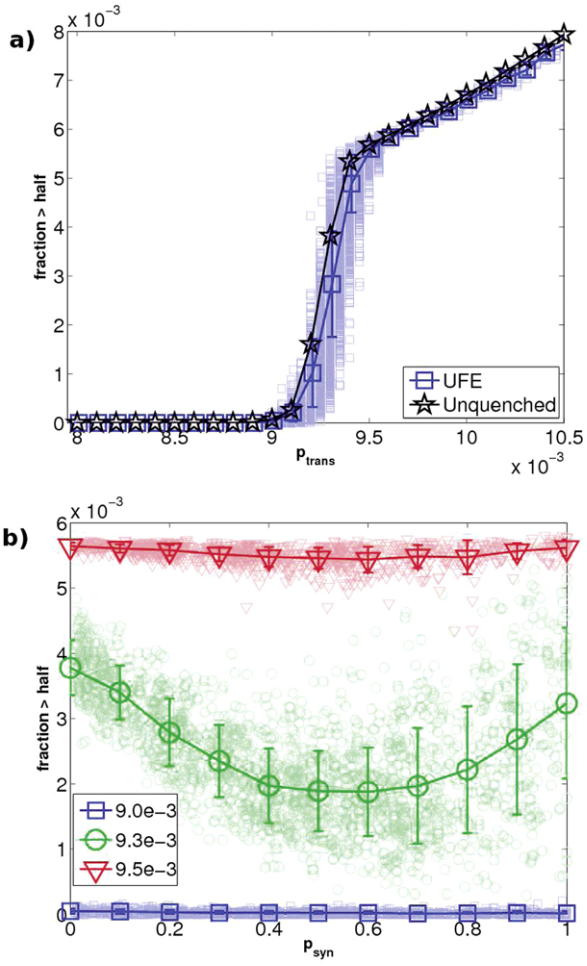

Fig. 9 (Color online) Frame (**a**): a comparison of $G_{\mathsf{UFE}}(N, M)$ and $G_{\mathsf{FULL}}(N)$. We have chosen 13,709 realizations of neuronal models with various M and p_{syn} and plotted these versus p_{trans}. Frame (**b**): effect of varying p_{syn} while holding p_{trans} constant where p_{trans} is held at $\{9.0, 9.3, 9.5\} \times 10^{-3}$ and we plot 1010, 1925, and 953 data points, respectively

Conditioning on p_{trans} determines the dynamics well (in the sense of the error bars being small in Figs. 8 and 9(a)), but we also see that there is some ensemble variance, especially in the intermediate range where synchronization is starting to appear. It is natural then to ask whether conditioning on more information might help predict the statistics of these models, and we explore this question in Fig. 9(b). Here, what we have done is taken the data in just three of the bins in Fig. 9(a) (specifically, the data corresponding to $p_{\mathsf{trans}} = \{9.0, 9.3, 9.5\} \times 10^{-3}$) and plotted these versus p_{syn}. Note that when p_{trans} is fixed, then M varies inversely proportionally to p_{syn}, so as one moves from left to right in Fig. 9(b), this corresponds to taking fewer edges but in such a way that $M p_{\mathsf{syn}}$ is held constant. The right-hand side of this graph corresponds to choosing $M = p_{\mathsf{trans}} N(N-1)$ synapses and making them perfectly reliable; whereas the left-hand edge corresponds to choosing a complete graph but making the synapses only work with probability p_{trans}. What we see is when synchronization is high or low, the dependence on p_{syn} is almost nonexistent, i.e., in the

high and low synchronization cases, the dynamics are mostly independent of p_{syn} and knowing the product $p_{\text{syn}}M$ is basically good enough to tell us everything.

In contrast, in the transition regime, knowing p_{syn} gives more information; interestingly, both the networks with the most, and the fewest, edges for a fixed p_{trans} tend to be most synchronous. However, it should be noted that specifying p_{syn} does not cut down ensemble variance that much: for example, in the $p_{\text{trans}} = 9.3 \times 10^{-3}$ data in Fig. 9(b), the standard deviation of all $p_{\text{trans}} = 9.3 \times 10^{-3}$ data is 9.35×10^{-4}, whereas the smallest error bar in that graph is 4.2×10^{-4}, i.e. the ensemble standard deviation after conditioning on $p_{\text{trans}} = 9.3 \times 10^{-3}$ and p_{syn} in the bin nearest zero only cuts down standard deviation by a factor of two.

Notice that in the middle regime, where the ensemble variance conditioned on p_{trans} is largest, and where p_{syn} plays a significant role, corresponds exactly to the switching regime of the network observed in DeVille and Peskin (2008), DeVille et al. (2010) where the all-to-all network has multiphase dynamics.

4 Detailed Study of Small World Models

In this section, we perform a detailed numerical study of the family of small world networks. We are studying small world models inspired by, and very similar to, those defined in Watts and Strogatz (1998). (The main differences are that we allow the graphs to be directed and we extend the definition to the case where the number of edges is not an integral multiple of the number of vertices.)

The main idea of the construction of the random model $G_{\text{SW}}(N, M, p_{\text{rewire}})$ is that we start with a very regular graph with N vertices and M edges (in fact, we make it as close to a bidirectional, locally-coupled ring as possible), and then rewire each edge with probability p_{rewire} (by "rewire" we mean remove an edge and replace it with an edge between a pair of vertices chosen uniformly at random). Thus, for p_{rewire} small, we have a regular and locally-coupled graph, but as $p_{\text{rewire}} \to 1$, we obtain the $G_{\text{UFE}}(N, M)$ model (if $p_{\text{rewire}} = 1$, we rewire every node, and thus every node is chosen uniformly at random).

Our major observations can be summarized as such:

- For p_{rewire} sufficiently large (which seems in practice to be the range of larger than 0.5), the model $G_{\text{SW}}(N, M, p_{\text{rewire}})$ is statistically almost the same as $G_{\text{UFE}}(N, M)$.
- For smaller p_{rewire}, the onset of synchronization is sharper as a function of p_{trans} and more severe. Thus, there is a "turn-around" phenomenon where the more regular graphs are less synchronous than the more random graphs at small p_{trans}, but become more synchronous for large p_{trans} (cf. Nishikawa et al. 2003).
- For smaller p_{rewire}, the ensemble variance is still rather large even after conditioning on p_{trans}; for larger p_{rewire} it is not. This means that in the class of more regular graphs, the details of the graph matter more.

4.1 Comparison of Statistics for Various p_{rewire}

In this subsection, we only present data where we have chosen $p_{\text{syn}} = 1$ but study the onset of synchronization versus both p_{rewire} and $p_{\text{trans}} = p_{\text{edge}} = M/(N(N-1))$.

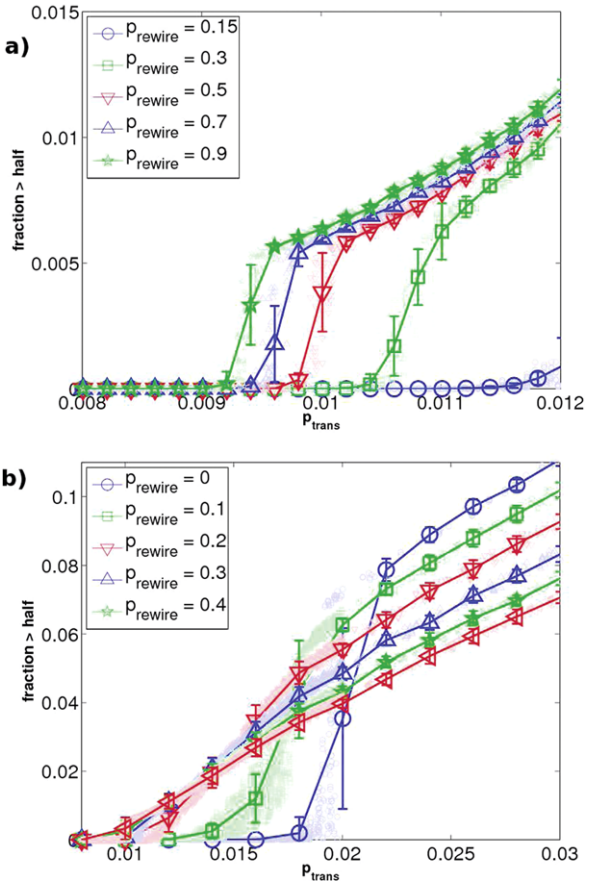

Fig. 10 (Color online) Synchronization as a function of $p_{\text{trans}} = p_{\text{edge}} = M/(N(N-1))$ for various p_{rewire}

In Fig. 10, each curve corresponds to a fixed p_{rewire}, and we show the effect of varying p_{trans}. We see that the large p_{rewire} give roughly the same shape, which are themselves very similar to the shape seen earlier for $G_{\text{FULL}}(N)$, $G_{\text{UP}}(N, p)$, $G_{\text{UFE}}(N, M)$, but smaller p_{trans} give much different shapes. As always, we plot the individual ensembles in the background, but show the bin mean and bin standard deviation for the curves.

In Fig. 11, we present this same data but collated in both heatmap and contour forms. It is clear in this figure that all $p_{\text{rewire}} > 1/2$ gives about the same synchronization, and that more regular graphs lag behind the more random graphs as p_{trans} is increased, but then catch up and even surpass them.

4.2 Varying p_{syn} for Fixed p_{trans} and p_{rewire}

In Fig. 12, we present the data in a similar manner to that shown in Fig. 9; each panel corresponds to choosing a fixed $p_{\text{rewire}} = 0.95, 0.75, 0.3$, or 0.1. Inside each panel, we choose high, medium, and low values of p_{trans} (the specific values are presented in Table 1). These values were chosen by eye from Fig. 10 to obtain values of p_{trans}

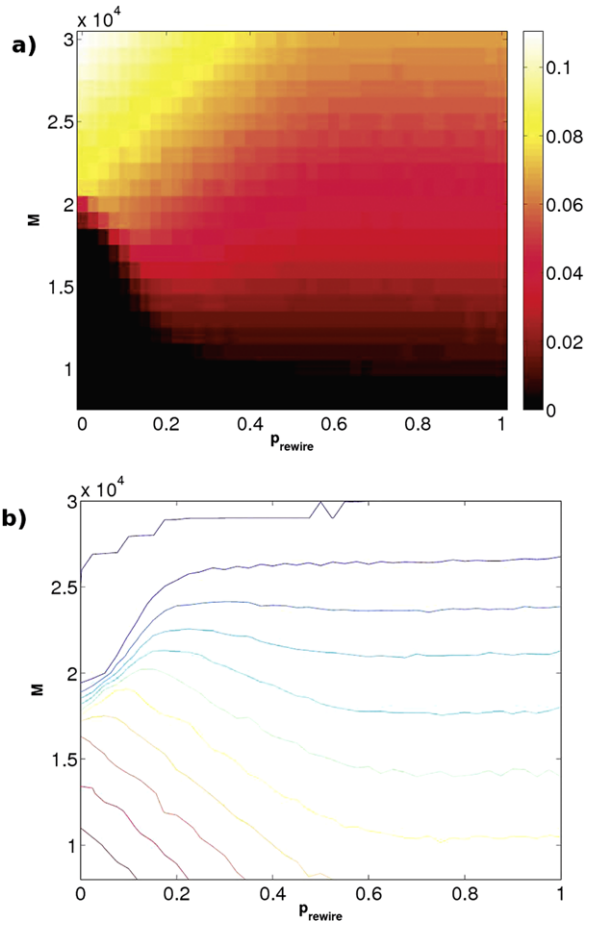

Fig. 11 (Color online) Data from Fig. 10 in heatmap and contour form

where the networks have high, medium, and low levels of synchronization. In each case, once p_{rewire} and p_{trans} have been fixed, we vary p_{syn} over the range $(p_{\text{trans}}, 1]$ and plot data as in Figs. 9(b) and 12. Again note that for fixed p_{trans}, we have M varying inversely proportionally to p_{syn}.

What is clear from these figures is, again, for larger p_{rewire}, the small world graphs act very much like $G_{\text{UFE}}(N, M)$; there is some dependence on p_{syn} once p_{trans} has been fixed, but it is not significant, as can be seen in Figs. 12(a, b). In short, for these p_{trans} is a good predictor. However, what we also see is that when p_{rewire} is small, fixing p_{trans} is not a good predictor. Considering Figs. 12(c, d), we see that not only does each curve have a large aggregate variance (i.e., fixing p_{trans} still has a large ensemble variance), further conditioning on p_{syn} makes a significant difference; as a function of p_{syn}, the binned variance is orders of magnitude less than the binned mean. This means that (for at least some values of p_{trans}) when p_{rewire} is small, conditioning on p_{syn} after conditioning on p_{trans} makes the prediction better by several orders of magnitude. This is in marked contrast to $G_{\text{UP}}(N, p)$, $G_{\text{UFE}}(N, M)$, or $G_{\text{SW}}(N, M, p_{\text{rewire}})$ with p_{rewire} large.

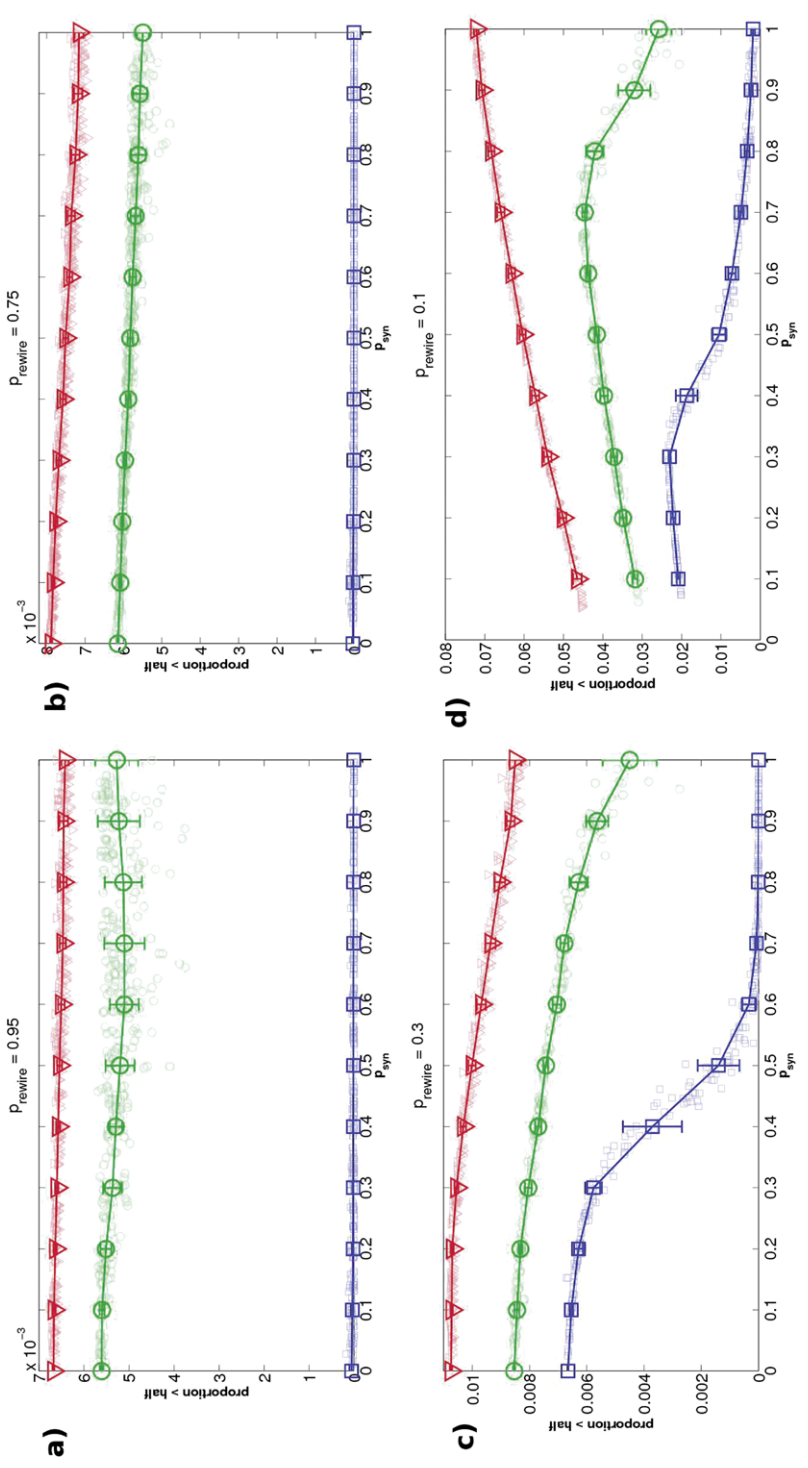

Fig. 12 *In each of these frames*, we fix a p_{rewire} (the values are $p_{\text{rewire}} = 0.95, 0.75, 0.3, 0.1$ in frames (**a–d**), respectively) and identify three values of p_{trans} corresponding to "low," "medium," and "high" synchrony (see Table 1) and then plot versus p_{syn} for fixed p_{rewire}, p_{trans}

Table 1 Values of p_{trans} chosen for each fixed p_{rewire}

p_{rewire}	Low	Medium	High
0.95	9×10^{-3}	9.5×10^{-3}	1×10^{-2}
0.75	9×10^{-3}	9.75×10^{-3}	1.05×10^{-2}
0.3	1×10^{-2}	1.075×10^{-2}	1.15×10^{-2}
0.1	1.4×10^{-2}	1.7×10^{-2}	2.2×10^{-2}

5 Detailed Study of Scale Free Models

In this section, we perform a more detailed analysis of scale-free models to elucidate some of the key features. As was observed in Figs. 5(d), 6(b), 7(b), the ensemble variance of the synchronization propensity of the network is significantly larger for the scale-free case than for the other cases. What this means is that fixing $p_{\text{trans}} = p_{\text{edge}} p_{\text{syn}}$ is not a very good predictor of synchronization.

One might ask for a sharper conditioning by conditioning on both p_{syn} and M and not just their product and see if this leads to a decrease in variance after such conditioning (this was the case for uniform and small-world graphs; see Figs. 9 and 12). It turns out that this is not the case, i.e., even if we proscribe a value of p_{syn} and a number of edges M, the dynamics of the networks drawn from the $G_{\text{SF}}(M, \alpha, \beta, \gamma)$ ensemble are significantly different.

We present one set of such data in Fig. 13. In this figure, we have chosen $M = 20000$ and $p_{\text{syn}} = 0.5$ throughout, but considered many different realizations of graphs from the $G_{\text{SF}}(20000, 0.25, 0.5, 0.25)$ ensemble. In each case, we have plotted the proportion of bursts larger than 20% of the network, i.e., those cascades that entrain more than 200 neurons.

We have chosen the 20% threshold here instead of the 50% threshold used in Sects. 3 and 4 for two reasons: first, this will allow us to obtain more data for the statistics, but more importantly, considering Fig. 3, we see that while the separation between small and large bursts is much less clear for the scale-free networks,if there is any separation between small and large bursts, it is closer to 20% of the network instead of 50%. In any case, we see in Fig. 5 that the ensemble variance conditioned on p_{trans} is large for either threshold.

The natural question to pose at this point is: if knowing the number of edges isn't enough to specify the dynamics of the network, is there some simple observable on which we can further condition to give us better predictions? Scale-free networks are inherently "hierarchical," i.e., that there are typically a few vertices in the graph with a large degree (Bollobás et al. 2003). In fact, this is the property of the network which gives rise to the term scale-free in the first place: the degree distribution is a power-law so that the probability of having vertices with high degree is non-zero. One might expect that knowing something about the vertex with highest degree, or a collection of vertices with highest degree (the "top-n vertices") might give us significant information about the dynamics on the network. We see in Fig. 13 that this is so. Here, we compute the fraction of cascades which entrain 20% of the network or more and plot this versus two observables of the graph. In Fig. 13(a), we plot this versus the highest in-degree in the graph. In all of these graphs, we have $M = 20000$ and

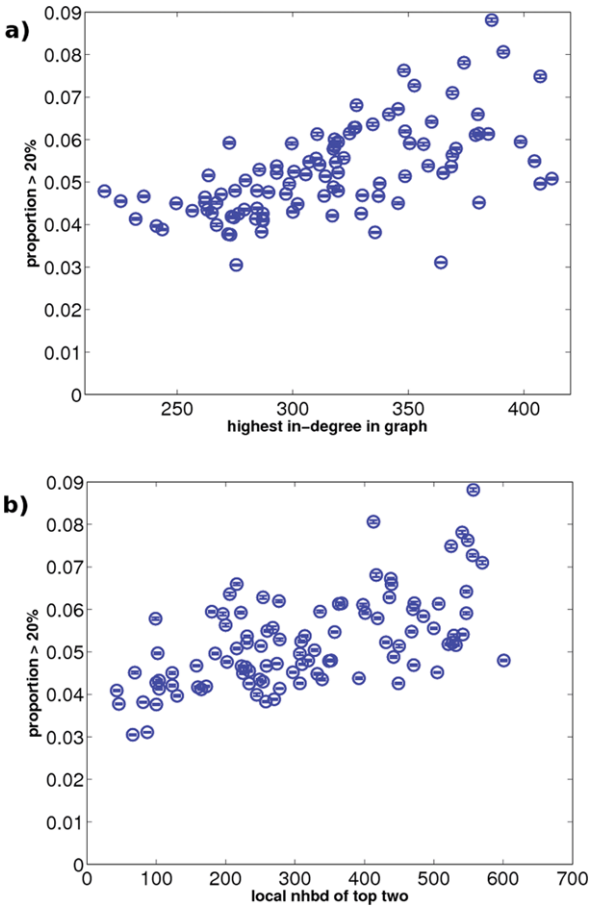

Fig. 13 All data here is for $G_{\mathsf{SF}}(20000, 1/4, 1/2)$ and we are plotting the proportion of cascades larger than 20% of the network. In panel (**a**), we plot these versus the in-degree of the neuron with the highest in-degree in the network, in panel (**b**) we plot these versus the size of the local neighborhood of the "top-2" vertices (see text for more detailed definitions)

$N = 1000$, so that the average in-degree is 20; the largest in-degree is thus somewhere between 10 and 20 times the average in-degree, but this the salient feature of scale-free networks. In Fig. 13(b), we are plotting versus a different statistic which we call the local neighborhood of the top two vertices. Specifically, what this means is that we choose the two neurons with largest in-degree and then count the total number of neurons on which they synapse; this is a proxy to understand the size of the network which the most connected neurons effect directly. More generally, we could define a top-n statistic as follows: define $d_{\mathsf{in}}(j) = \#\{i \mid i \to j\}$ and renumber the vertices in increasing order of $d_{\mathsf{in}}(\cdot)$, and then our statistic is

$$N_k(G) = \sum_{j=N-k+1}^{N} \#\{\ell \mid j \to \ell\},$$

and we count vertices multiple times if they appear multiple times in this sum. The statistic we have chosen in Fig. 13(b) is $N_2(G)$. We see that in both cases these statistics give useful information in the sense that there is a clear positive correlation

in both of these graphs, but neither statistic completely specifies. We also compared to $N_k(G)$ for $k = 3, \ldots, 10$ (which data we do not present here) but found quite similar results.

The next question one might ask is why in-degree is presented here, as we could have easily have presented this data versus the highest out-degree in the graph instead. We could define "in-hubs" as those vertices with large in-degree and "out-hubs" as those with large out-degree and then ask why in-hubs over out-hubs?

What we find is perhaps somewhat surprising, and that is that looking at in-hubs gives significantly better predictive powers than looking at out-hubs. One can pose the following question: which neurons are involved in the synchronous events, i.e., whenever we consider cascades which take over 20% or more of the network, which neurons are most likely to take part in these events? And are these neurons more or less likely to be hubs than not?

To explore this question, we perform the following computation.

Definition 5 Given a function $f\colon V(G) \to \mathbb{R}$ on the vertices of G, we define a *ranking* as any permutation $\pi \in S_{|G|}$ which makes $f \circ \pi$ an increasing function (i.e. π_1 is the vertex with smallest value of f, and π_N is the vertex with the largest value of f). Such a permutation always exists but of course may not be unique. We then define the set

$$S_{f,n}(G) = \pi\big([k, N]\big), \quad k = \min_{\ell} f(\pi_\ell) = f(\pi_{N-n+1}),$$

where π is any ranking permutation for f. This set is unique.

Thus for any function f, and graph G, $S_{f,n}(G)$ identifies the "top-n" vertices for that particular function, i.e., the n vertices that have the largest value of f. Notice that we also include the possibilities of "ties," so that the top-n vertices for a function might include some number $\geq n$; if, for example, $f(\pi_{N-3}) = f(\pi_{N-4})$, then both the top-4 and the top-5 sets contain at least the five vertices $\pi([N-4, N])$.

We define $d_{\text{in}}(j)$ as above, $d_{\text{out}}(j)$ similarly, and $Q(j)$ as the fraction of cascades larger than 20% in which neuron j fired. For each the networks present in Fig. 13, and for $n = 1, \ldots, 500$, we identified the three sets $S_{\text{in},n}(G)$, $S_{\text{out},n}(G)$, and $S_{Q,n}(G)$ (we abuse notation a bit by denoting $S_{\text{in},n}(G)$ as the sets corresponding to the function d_{in}, and similarly for $S_{\text{out},n}(G)$ and d_{out}, to simplify subscripts).

The idea here is the sets $S_{Q,n}$ characterize which neurons are taking place in the large cascades, and $S_{\text{in},n}(G)$, $S_{\text{out},n}(G)$ are identifying which neurons are in-hubs and out-hubs in the graph-theoretic sense. We then compute two functions

$$\varphi^G_{\text{in}}(n) = \frac{|S_{\text{in},n}(G) \cap S_{Q,n}(G)|}{\min(|S_{\text{in},n}(G)|, |S_{Q,n}(G)|)}, \qquad \varphi^G_{\text{out}}(n) = \frac{|S_{\text{out},n}(G) \cap S_{Q,n}(G)|}{\min(|S_{\text{out},n}(G)|, |S_{Q,n}(G)|)}.$$

(Note that we actually need to specify the terms in the denominator since these sets have sizes $\geq n$.) The functions φ will vary between 0 and 1; a value of 0 means the sets have empty intersection and a value of 1 means they coincide. Larger values mean the sets share more in common and when these values are high it suggests a correlation between the properties. Of course, as $n \to N$, these values will all approach 1 so they are only significant when n is not too close to N.

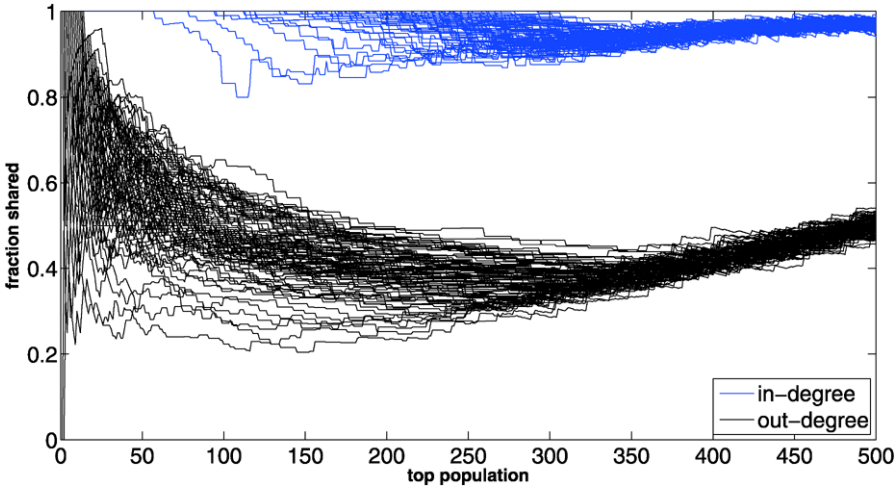

Fig. 14 The quantities $\varphi_{\mathsf{in}}^{G}(n)$ and $\varphi_{\mathsf{out}}^{G}(n)$ plotted versus n. *Each curve* corresponds to a single realization of G from $G_{\mathsf{SW}}(1000, 20000, 1/4, 1/2)$, each of which corresponds to one of the data points in Fig. 13

We plot these two functions, $\varphi_{\mathsf{in}}(n)$ and $\varphi_{\mathsf{out}}(n)$, in Fig. 14. In short, these pictures show clearly that the in-hubs participate more in the synchronous dynamics than the out-hubs, we see that the list of top in-hubs and top synchronous neurons share about 90% of their members in most cases and dominate the out-hubs significantly. As a concrete example, let us say that we wanted to predict the 100 most active neurons in a given scale-free graph. Simply choosing the top 100 in-hubs would, aside from four particular graphs, give us exactly the top 100 active neurons, and even in those four bad cases we would have a large degree of overlap. Said differently, for all but four of these graphs, $\varphi_{\mathsf{in}}(100) = 1$, and in any case is never lower than 80%. Conversely, choosing the 100 largest out-hubs would give us coverage ranging from 20%–60%.

6 Conclusions

We have demonstrated a wide variety of phenomenological behavior of neuronal network dynamics on complex graphs. A brief summary, almost a mnemonic, of these results is:

> Uniform and small-world graphs are almost just like all-to-all networks but scale-free networks are quite different. The fine structure of the uniform and scale-free networks does not seem to matter much, but the fine details of the scale-free networks matter quite a bit.

More precisely, we have shown

- For $G_{\mathsf{UP}}(N, p)$, $G_{\mathsf{UFE}}(N, M)$ and away from the "switching regime," the single parameter p_{trans} is a good descriptor of the synchronization properties of the network, and these networks look like $G_{\mathsf{FULL}}(N)$. These statements hold for $G_{\mathsf{SW}}(N, M, p_{\mathsf{rewire}})$ as well when $p_{\mathsf{rewire}} > 0.5$.

- $G_{\mathsf{SF}}(N, M, \alpha, \beta)$ acts nothing like these other graphs: the onset of synchronization happens over a much larger range of p_{trans} and the ensemble variance conditioned on p_{trans} is much larger. Moreover, even conditioning on p_{syn} and M separately gives a large ensemble variance. The main reason for this is that the local structure near the hubs of the network are very important, yet the variance of this local structure is large, even after conditioning on M.

Acknowledgements The authors are indebted to Josh Attenberg, Joszef Balogh, Brent Doiron, and Joel Spencer for discussion which stimulated this work.

Appendix: Algorithmic Descriptions of Random Graphs

We have used the random graphs $G_{\mathsf{UP}}(N, p)$, $G_{\mathsf{UFE}}(N, M)$, $G_{\mathsf{SW}}(N, M, p_{\mathsf{rewire}})$, and $G_{\mathsf{SF}}(N, M, \alpha, \beta)$, which we now define precisely.

- $G_{\mathsf{UP}}(N, p)$—Given a graph with N vertices, there are $N(N-1)$ possible directed edges. We take each one to be present independently with probability p, i.e., say $e_{ij} = 1$ with probability p for all i, j. The number of edges in this graph is the Bernoulli random variable with $N(N-1)$ trials and probability p of success and, therefore, the expected value of the number of edges is $N(N-1)p$.
- $G_{\mathsf{UFE}}(N, M)$—This graph has exactly M edges, in contrast to $G_{\mathsf{UP}}(N, p)$. Start with the empty graph, and add edges to the graph by picking two vertices, each with probability N^{-1}, and add the directed edge between them. If this edge already exists, do nothing. Repeat until the graph has M edges.
- $G_{\mathsf{SW}}(N, M, p_{\mathsf{rewire}})$—This graph, like $G_{\mathsf{UFE}}(N, M)$, has N vertices and M edges. For each of the M edges, with probability p_{rewire}, we place the edge randomly as in $G_{\mathsf{UFE}}(M, N)$. With probability $1 - p_{\mathsf{rewire}}$, we choose the edge to connect vertex $M \pmod N$ and $M + \lfloor M/N \rfloor \pmod N$. We pick the source of this edge to be one of these vertices, with probability $1/2$. To compare this definition to that of Watts and Strogatz (1998), consider the case where $p_{\mathsf{rewire}} = 0$, $M = kN$. Here, each vertex is connected to exactly its k closest neighbors (with random directionality). With $p_{\mathsf{rewire}} > 0$, some of the edges become not near-neighbor because of a "rewiring"; one way to think of this is to connect each vertex to its M nearest neighbors on each side, and then rewire each connection with probability p_{rewire}. In particular, if $M = kN$, then this is exactly the model of Watts and Strogatz (1998) except that we allow directed edges.
- $G_{\mathsf{SF}}(N, M, \alpha, \beta)$—We use a slight modification of the scale-free model presented in Bollobás et al. (2003). One choice of the model presented there is as follows: Start with a graph with one vertex. At each step, we do one of three things: with probability α we add a new vertex and an edge from the new vertex to an existing vertex, with probability β add a new edge between existing vertices, and with probability $(1 - \alpha - \beta)$ add a new vertex and an edge from an existing vertex to the new one. Which existing vertex we choose in each case is random and determined by the following probability distribution: if we add an edge coming into an existing vertex, the probability of choosing vertex v_j is proportional to $1 + d_{\mathsf{in},j}$, its in-degree plus one, and if we add an edge leaving an existing vertex, the probability of choosing vertex v_j is proportional to $1 + d_{\mathsf{out},j}$, its out-degree plus one.

Since each step always adds one edge, we can fix the number of edges at M by performing exactly $M - 1$ steps. However, the number of vertices in this graph will be random with mean $\alpha(1 - \alpha - \beta)M$. Since we also want to have a graph with exactly N vertices, we force the graph to have N vertices: if during the evolution of the random graph as described above, we end up with N vertices, then we stop adding vertices but continue to add edges between existing vertices as described above, i.e., set $\alpha = 0, \beta = 1$. If α, β are chosen, for example, larger than $1.1N$, then for N large enough it is exponentially unlikely that this algorithm terminates before N vertices are chosen (in practice, we check for this and if this happens, reject the graph).

References

Abbott, L. F., & van Vreeswijk, C. (1993). Asynchronous states in networks of pulse-coupled oscillators. *Phys. Rev. E*, *48*(2), 1483–1490.

Abrams, D. M., Mirollo, R., Strogatz, S. H., & Wiley, D. A. (2008). Solvable model for chimera states of coupled oscillators. *Phys. Rev. Lett.*, *101*(8), 084103.

Albert, R., & Barabási, A.-L. (2002). Statistical mechanics of complex networks. *Rev. Mod. Phys.*, *74*(1), 47–97.

Alon, N., & Spencer, J.H. (2008). *Wiley-Interscience series in discrete mathematics and optimization*. *The probabilistic method* (3rd ed.). Hoboken: Wiley. With an appendix on the life and work of Paul Erdős.

Apfaltrer, F., Ly, C., & Tranchina, D. (2006). Population density methods for stochastic neurons with realistic synaptic kinetics: firing rate dynamics and fast computational methods. *Network, Comput. Neural Syst.*, *17*(4), 373–418.

Arenas, A., Díaz-Guilera, A., Kurths, J., Moreno, Y., & Zhou, C. (2008). Synchronization in complex networks. *Phys. Rep.*, *469*(3), 93–153.

Barabási, A.-L., & Albert, R. (1999). Emergence of scaling in random networks. *Science*, *286*(5439), 509–512.

Barahona, M., & Pecora, L. M. (2002). Synchronization in small-world systems. *Phys. Rev. Lett.*, *89*(5), 054101.

Bascompte, J. (2007). Networks in ecology. *Basic Appl. Ecol.*, *8*(6), 485–490.

Beggs, J. M., & Plenz, D. (2003). Neuronal avalanches in neocortical circuits. *J. Neurosci.*, *23*(35), 11167–11177.

Beggs, J. M., & Plenz, D. (2004). Neuronal avalanches are diverse and precise activity patterns that are stable for many hours in cortical slice cultures. *J. Neurosci.*, *24*(22), 5216–5229.

Bhan, A., Galas, D. J., & Dewey, T. G. (2002). A duplication growth model of gene expression networks. *Bioinformatics*, *18*(11), 1486–1493.

Boccaletti, S., Latora, V., Moreno, Y., Chavez, M., & Hwang, D.-U. (2006). Complex networks: structure and dynamics. *Phys. Rep.*, *424*(4–5), 175–308.

Bollobás, B. (2001). *Cambridge studies in advanced mathematics*: *Vol. 73*. *Random graphs* (2nd ed.). Cambridge: Cambridge University Press.

Bollobás, B., Borgs, C., Chayes, J., & Riordan, O. (2003). Directed scale-free graphs. In *Proceedings of the fourteenth annual ACM-SIAM symposium on discrete algorithms* (pp. 132–139), Baltimore, MD, 2003. New York: ACM.

Bower, J. M., & Bolouri, H. (Eds.) (2001). *Computational modeling of genetic and biochemical networks*. Cambridge: MIT Press.

Bressloff, P. C., & Coombes, S. (1998a). Traveling waves in a chain of pulse-coupled oscillators. *Phys. Rev. Lett.*, *80*(21), 4815–4818.

Bressloff, P. C., & Coombes, S. (1998b). Desynchronization, mode locking, and bursting in strongly coupled integrate-and-fire oscillators. *Phys. Rev. Lett.*, *81*(10), 2168–2171.

Bressloff, P. C., & Coombes, S. (1998c). Desynchronization, mode locking, and bursting in strongly coupled integrate-and-fire oscillators. *Phys. Rev. Lett.*, *81*(10), 2168–2171.

Bressloff, P. C., & Coombes, S. (2000). A dynamical theory of spike train transitions in networks of integrate-and-fire oscillators. *SIAM J. Appl. Math.*, *60*(3), 820–841 (electronic).

Bressloff, P. C., Coombes, S., & de Souza, B. (1997). Dynamics of a ring of pulse-coupled oscillators: group-theoretic approach. *Phys. Rev. Lett.*, *79*(15), 2791–2794.

Brunel, N., & Hakim, V. (1999). Fast global oscillations in networks of integrate-and-fire neurons with low firing rates. *Neural Comput.*, *11*(7), 1621–1671.

Cai, D., Tao, L., Shelley, M., & McLaughlin, D. W. (2004). An effective kinetic representation of fluctuation-driven neuronal networks with application to simple and complex cells in visual cortex. *Proc. Natl. Acad. Sci. USA*, *101*(20), 7757–7762.

Cai, D., Tao, L., Rangan, A. V., & McLaughlin, D. W. (2006). Kinetic theory for neuronal network dynamics. *Commun. Math. Sci.*, *4*(1), 97–127.

Campbell, S. R., Wang, D. L. L., & Jayaprakash, C. (1999). Synchrony and desynchrony in integrate-and-fire oscillators. *Neural Comput.*, *11*(7), 1595–1619.

Dayan, P., & Abbott, L. F. (2001). *Theoretical neuroscience: computational and mathematical modeling of neural systems*. Cambridge: MIT Press.

Dellnitz, M., Golubitsky, M., Hohmann, A., & Stewart, I. (1995). Spirals in scalar reaction-diffusion equations. *Int. J. Bifurc. Chaos Appl. Sci. Eng.*, *5*(6), 1487–1501.

DeVille, R. E. L., & Peskin, C.S. (2008). Synchrony and asynchrony in a fully stochastic neural network. *Bull. Math. Biol.*, *70*(6), 1608–1633.

DeVille, R. E. L., Peskin, C. S., & Spencer, J. H. (2010). Dynamics of stochastic neuronal networks and the connections to random graph theory. *Math. Model. Nat. Process.*, *5*(2), 26–66.

Dionne, B., Golubitsky, M., Silber, M., & Stewart, I. (1995). Time-periodic spatially periodic planforms in Euclidean equivariant partial differential equations. *Philos. Trans. R. Soc. Lond., Ser. A*, *352*(1698), 125–168.

Dionne, B., Golubitsky, M., & Stewart, I. (1996a). Coupled cells with internal symmetry. I. Wreath products. *Nonlinearity*, *9*(2), 559–574.

Dionne, B., Golubitsky, M., & Stewart, I. (1996b). Coupled cells with internal symmetry. II. Direct products. *Nonlinearity*, *9*(2), 575–599.

Erdős, P., & Rényi, A. (1959). On random graphs. I. *Publ. Math. (Debr.)*, *6*, 290–297.

Erdős, P., & Rényi, A. (1960). On the evolution of random graphs. *Magy. Tud. Akad. Mat. Kut. Intéz. Közl.*, *5*, 17–61.

Eurich, C. W., Herrmann, J. M., & Ernst, U. A. (2002). Finite-size effects of avalanche dynamics. *Phys. Rev. E*, *66*(6), 066137.

Field, M., Golubitsky, M., & Stewart, I. (1991). Bifurcations on hemispheres. *J. Nonlinear Sci.*, *1*(2), 201–223.

Gerstner, W., & van Hemmen, J. L. (1993). Coherence and incoherence in a globally-coupled ensemble of pulse-emitting units. *Phys. Rev. Lett.*, *71*(3), 312–315.

Goel, P., & Ermentrout, B. (2002). Synchrony, stability, and firing patterns in pulse-coupled oscillators. *Phys. D, Nonlinear Phenom.*, *163*(3–4), 191–216.

Golubitsky, M., & Stewart, I. (1984). Hopf bifurcation in the presence of symmetry. *Bull. Am. Math. Soc.*, *11*(2), 339–342.

Golubitsky, M., & Stewart, I. (1985). Hopf bifurcation in the presence of symmetry. *Arch. Ration. Mech. Anal.*, *87*(2), 107–165.

Golubitsky, M., & Stewart, I. (1986a). Hopf bifurcation with dihedral group symmetry: coupled nonlinear oscillators. In *Contemp. math.: Vol.* 56. *Multiparameter bifurcation theory*, Arcata, Calif., 1985 (pp. 131–173). Providence: Am. Math. Soc.

Golubitsky, M., & Stewart, I. (1986b). Symmetry and stability in Taylor-Couette flow. *SIAM J. Math. Anal.*, *17*(2), 249–288.

Golubitsky, M., & Stewart, I. (1987). Generic bifurcation of Hamiltonian systems with symmetry. *Physica D*, *24*(1–3), 391–405. With an appendix by Jerrold Marsden.

Golubitsky, M., & Stewart, I. (1999a). Symmetry and pattern formation in coupled cell networks. In *IMA Math. Appl.: Vol.* 115. *Pattern formation in continuous and coupled systems* (pp. 65–82), Minneapolis, MN, 1998. New York: Springer.

Golubitsky, M., & Stewart, I. (1999b). Symmetry and pattern formation in coupled cell networks. In *IMA Vol. Math. Appl.: Vol.* 115. *Pattern formation in continuous and coupled systems* (pp. 65–82), Minneapolis, MN, 1998. New York: Springer.

Golubitsky, M., & Stewart, I. (2002a). *Progress in mathematics*: *Vol.* 200. *The symmetry perspective*. Basel: Birkhäuser. From equilibrium to chaos in phase space and physical space.

Golubitsky, M., & Stewart, I. (2002b). Patterns of oscillation in coupled cell systems. In *Geometry, mechanics, and dynamics* (pp. 243–286). New York: Springer.

Golubitsky, M., & Stewart, I. (2002c). *Progress in mathematics*: Vol. 200. *The symmetry perspective*. Basel: Birkhäuser. From equilibrium to chaos in phase space and physical space.
Golubitsky, M., & Stewart, I. (2005). Synchrony versus symmetry in coupled cells. In *EQUADIFF* (pp. 13–24), World Sci. Publ., Hackensack.
Golubitsky, M., & Stewart, I. (2006). Nonlinear dynamics of networks: the groupoid formalism. *Bull. Am. Math. Soc.*, *43*(3), 305–364.
Golubitsky, M., Stewart, I., & Schaeffer, D. G. (1988). *Applied mathematical sciences*: *Vol.* 69. *Singularities and groups in bifurcation theory, Vol. II*. New York: Springer.
Golubitsky, M., Stewart, I., & Dionne, B. (1994). Coupled cells: wreath products and direct products. In *NATO Adv. Sci. Inst. Ser. C Math. Phys. Sci.: Vol.* 437. *Dynamics, bifurcation and symmetry*, Cargèse, 1993 (pp. 127–138). Dordrecht: Kluwer Academic.
Golubitsky, M., Stewart, I., Buono, P.-L., & Collins, J. J. (1998). A modular network for legged locomotion. *Physica D*, *115*(1–2), 56–72.
Golubitsky, M., Knobloch, E., & Stewart, I. (2000). Target patterns and spirals in planar reaction-diffusion systems. *J. Nonlinear Sci.*, *10*(3), 333–354.
Golubitsky, M., Nicol, M., & Stewart, I. (2004a). Some curious phenomena in coupled cell networks. *J. Nonlinear Sci.*, *14*(2), 207–236.
Golubitsky, M., Pivato, M., & Stewart, I. (2004b). Interior symmetry and local bifurcation in coupled cell networks. *Dyn. Syst.*, *19*(4), 389–407.
Golubitsky, M., Stewart, I., & Török, A. (2005). Patterns of synchrony in coupled cell networks with multiple arrows. *SIAM J. Appl. Dyn. Syst.*, *4*(1), 78–100 (electronic).
Golubitsky, M., Josić, K., & Shea-Brown, E. (2006). Winding numbers and average frequencies in phase oscillator networks. *J. Nonlinear Sci.*, *16*(3), 201–231.
Golubitsky, M., Shiau, L., & Stewart, I. (2007). Spatiotemporal symmetries in the disynaptic canal-neck projection. *SIAM J. Appl. Math.*, *67*(5), 1396–1417 (electronic).
Hansel, D., Mato, G., & Meunier, C. (1993). Clustering and slow switching in globally coupled phase oscillators. *Phys. Rev. E*, *48*(5), 3470–3477.
Haskell, E., Nykamp, D. Q., & Tranchina, D. (2001). Population density methods for large-scale modelling of neuronal networks with realistic synaptic kinetics: cutting the dimension down to size. *Network, Comput. Neural Syst.*, *12*(2), 141–174.
Hong, H., Choi, M. Y., & Kim, B. J. (2002). Synchronization on small-world networks. *Phys. Rev. E*, *65*(2), 026139.
Huygens, C. (1673). *Horoloquium oscilatorium*. Paris: Parisiis.
Janson, S., Łuczak, T., & Rucinski, A. (2000). *Wiley-Interscience series in discrete mathematics and optimization*. *Random graphs*. New York: Wiley-Interscience.
Knight, B. W. (1972). Dynamics of encoding in a population of neurons. *J. Gen. Physiol.*, *59*(6), 734–766.
Kuramoto, Y. (1984). *Springer series in synergetics*: *Vol.* 19. *Chemical oscillations, waves, and turbulence*. Berlin: Springer.
Kuramoto, Y. (1991). Collective synchronization of pulse-coupled oscillators and excitable units. *Physica D*, *50*(1), 15–30.
Lago-Fernández, L. F., Huerta, R., Corbacho, F., & Sigüenza, J. A. (2000). Fast response and temporal coherent oscillations in small-world networks. *Phys. Rev. Lett.*, *84*(12), 2758–2761.
Leclerc, R. D. (2008). Survival of the sparsest: robust gene networks are parsimonious. *Molecular Systems Biology*, *4*(213).
Levina, A., Herrmann, J. M., & Geisel, T. (2007). Dynamical synapses causing self-organized criticality in neural networks. *Nat. Phys.*, *3*, 857–960.
Levina, A., Herrmann, J. M., & Geisel, T. (2009). Phase transitions towards criticality in a neural system with adaptive interactions. *Phys. Rev. Lett.*, *102*(11), 118110.
Lindner, B., García-Ojalvo, J., Neiman, A., & Schimansky-Geier, L. (2004). Effects of noise in excitable systems. *Phys. Rep.*, *392*(6), 321–424.
Milo, R., Shen-Orr, S., Itzkovitz, S., Kashtan, N., Chklovskii, D., & Alon, U. (2002). Network motifs: simple building blocks of complex networks. *Science*, *298*(5594), 824–827.
Mirollo, R. E., & Strogatz, S. H. (1990). Synchronization of pulse-coupled biological oscillators. *SIAM J. Appl. Math.*, *50*(6), 1645–1662.
Mirollo, R. E., & Strogatz, S. H. (2005). The spectrum of the locked state for the Kuramoto model of coupled oscillators. *Phys. D, Nonlinear Phenom.*, *205*(1–4), 249–266. Synchronization and pattern formation in nonlinear systems: new developments and future perspectives.
Mirollo, R., & Strogatz, S. H. (2007). The spectrum of the partially locked state for the Kuramoto model. *J. Nonlinear Sci.*, *17*, 309–347. 10.1007/s00332-006-0806-x.

Newman, M. E. J. (2003). The structure and function of complex networks. *SIAM Rev.*, *45*(2), 167–256 (electronic).

Nishikawa, T., Motter, A. E., Lai, Y.-C., & Hoppensteadt, F. C. (2003). Heterogeneity in oscillator networks: are smaller worlds easier to synchronize? *Phys. Rev. Lett.*, *91*(1), 014101.

Peskin, C. S. (1975). *Mathematical aspects of heart physiology*. New York: Courant Institute of Mathematical Sciences New York University. Notes based on a course given at New York University during the year 1973/1974. See http://math.nyu.edu/faculty/peskin/heartnotes/index.html.

Pikovsky, A., Rosenblum, M., & Kurths, J. (2003). *Synchronization: a universal concept in nonlinear sciences*. Cambridge: Cambridge University Press.

Schlitt, T., & Brazma, A. (2007). Current approaches to gene regulatory network modelling. *BMC Bioinformatics*, *8*(6).

Senn, W., & Urbanczik, R. (2000/2001). Similar nonleaky integrate-and-fire neurons with instantaneous couplings always synchronize. *SIAM J. Appl. Math.*, *61*(4), 1143–1155 (electronic).

Shmulevich, I., Dougherty, E. R., Kim, S., & Zhang, W. (2002). Probabilistic boolean networks: a rule-based uncertainty model for gene regulatory networks. *Bioinformatics*, *18*(2), 261–274.

Sirovich, L. (2003). Dynamics of neuronal populations: eigenfunction theory; some solvable cases. *Network, Comput. Neural Syst.*, *14*(2), 249–272.

Sirovich, L., Omrtag, A., & Knight, B. W. (2000). Dynamics of neuronal populations: the equilibrium solution. *SIAM J. Appl. Math.*, *60*(6), 2009–2028.

Stewart, I., Golubitsky, M., & Pivato, M. (2003). Symmetry groupoids and patterns of synchrony in coupled cell networks. *SIAM J. Appl. Dyn. Syst.*, *2*(4), 609–646 (electronic).

Strogatz, S. (2003). *Sync: the emerging science of spontaneous order*. New York: Hyperion.

Terman, D., Kopell, N., & Bose, A. (1998). Dynamics of two mutually coupled slow inhibitory neurons. *Physica D*, *117*(1–4), 241–275.

Tsodyks, M., Mitkov, I., & Sompolinsky, H. (1993). Pattern of synchrony in inhomogeneous networks of oscillators with pulse interactions. *Phys. Rev. Lett.*, *71*(8), 1280–1283.

van Vreeswijk, C., Abbott, L., & Ermentrout, G. (1994). When inhibition not excitation synchronizes neural firing. *J. Comput. Neurosci.*, 313–322.

Watts, D. J., & Strogatz, S. H. (1998). Collective dynamics of 'small-world' networks. *Nature*, *393*(6684), 440–442.

Wilkinson, D. J. (2006). *Stochastic modelling for systems biology*. *Chapman & Hall/CRC mathematical and computational biology series*. Boca Raton: Chapman & Hall/CRC.

Winfree, A. T. (2001). *The geometry of biological time*. *Interdisciplinary applied mathematics* (2nd ed., *Vol.* 12). New York: Springer.

Zhao, F., Yang, H., & Wang, B. (2005). Scaling invariance in spectra of complex networks: a diffusion factorial moment approach. *Phys. Rev. E*, *72*(4), 046119.